



1 Impacts of soil management and climate on saturated
2 and near-saturated hydraulic conductivity: analyses of
3 the Open Tension-disk Infiltrometer Meta-database
4 (OTIM)

5 **Authors**

6 Guillaume Blanchy¹, Lukas Albrecht², Gilberto Bragato³, Sarah Garré¹, Nicholas Jarvis⁴, John Koestel^{2,4}

7

8 ¹*Flanders Research Institute for Agriculture, Fisheries and Food (ILVO), Melle, Belgium*

9 ²*Agroscope, Reckenholzstrasse 191, 8046 Zürich, Switzerland*

10 ³*Council for Agricultural Research and Economics (CREA), Via Po, 14, 00198 Roma, Italy*

11 ⁴*Department of Soil and Environment, Swedish University of Agricultural Sciences (SLU), P.O. Box 7014, 750 07*
12 *Uppsala, Sweden*

13

14 **Corresponding author**

15 John Koestel (johannes.koestel@agroscope.admin.ch)

16

17 **Keywords**

18 hydraulic conductivity, saturated hydraulic conductivity K_s , near-saturated hydraulic conductivity,
19 Kunsat, Knearsat, soil hydraulic properties, infiltration, tension-disk infiltrometer, soil properties, climate,
20 soil, agricultural management practice, pedo-climatic factors, meta-analysis

21 **Abstract**

22 Saturated and near-saturated soil hydraulic conductivities K_h ($\text{mm}\cdot\text{h}^{-1}$) determine the partitioning of
23 precipitation into surface runoff and infiltration and are fundamental to soils' susceptibility to preferential
24 flow. Recent studies have found indications that climate factors influence K_h , which is highly relevant in
25 the face of climate change. In this study, we investigated relationships between pedo-climatic factors



26 and K_r and also evaluated effects of land use and soil management. To this end, we collated the Open
27 Tension-disk Infiltrometer Meta-database (OTIM), which contains 1297 individual data entries from 172
28 different publication sources. We analysed a spectrum of saturated and near-saturated hydraulic
29 conductivities at matric potentials between 0 to 100 mm. We found that methodological details like the
30 direction of the wetting sequence or the choice of method for calculating infiltration rates to hydraulic
31 conductivities had a large impact on the results. We therefore restricted ourselves to a subset of 466 of
32 the 1297 data entries with similar methodological approaches. Correlations between K_s and K_r at higher
33 supply tensions decreased especially close to saturation, indicating a different flow mechanism at and
34 very close to saturation as towards the dry end of the investigated tension range. Climate factors were
35 better correlated to topsoil near-saturated hydraulic conductivities at supply tensions ≥ 30 mm than soil
36 texture, bulk density and organic carbon content. We find it most likely that the climate variables are
37 proxies for soil macropore networks created by respective biological activity, pedogenesis and climate
38 specific land use and management choices. Due to incomplete documentation in the source
39 publications of OTIM, we could investigate only a few land use types and agricultural management
40 practices. Land use, tillage system and soil compaction significantly influenced K_r , with effect sizes
41 appearing comparable to the ones of soil texture and soil organic carbon. The data in OTIM show
42 experimental bias is present, introduced by the choice of measurement time relative to soil tillage,
43 experimental design or data evaluation procedures. The establishment of best-practice rules for
44 tension-disk infiltrometer measurements would therefore be helpful. Future studies are needed to
45 investigate how climate shapes soil macropore networks and how land use and management can be
46 adapted to improve soil hydraulic properties. Both tasks require large amounts of new measurement
47 data with improved documentation on soil biology and land use and management history.

48 1. Introduction

49 Climate models predict more frequent extreme weather events such as high intensity rainfall with the
50 onset of global warming. To prevent water runoff and erosion, soils need to be able to conduct
51 sometimes large amounts of water in a short time. It is generally accepted that one key soil property is
52 the saturated hydraulic conductivity K_s ($\text{mm}\cdot\text{h}^{-1}$), as it determines the partitioning of precipitation into



53 surface runoff and infiltration. A large K_s reduces erosion risks and allows water to infiltrate into deeper
54 soil layers, where it may replenish an important reservoir of plant available water or contribute to
55 groundwater recharge. The hydraulic conductivity of a soil decreases with decreasing water content,
56 i.e. with decreasing water saturation. The hydraulic conductivity in the so-called near-saturated range
57 (between 0 and 100 mm matric tensions) is likewise important. Soils with larger near-saturated hydraulic
58 conductivity K_r ($\text{mm}\cdot\text{h}^{-1}$) tend to generate less water flow in macropore networks. Therefore, they are
59 less susceptible to preferential flow (Larsbo et al., 2014) by which agrochemicals and other solutes
60 quickly leach towards the groundwater. Moreover, a large K_r also indicates a well-aerated soil, which
61 drains faster and helps air to escape the soil in case of heavy rainfall. This further reduces the risk of
62 surface runoff and erosion as entrapped air strongly decreases soil hydraulic conductivity.

63 Saturated hydraulic conductivity is measured either in the laboratory on small cylinders, usually with
64 diameters < 7 cm (Klute & Dirksen, 1985) or it is acquired from field measurements, either using single
65 or double ring methods (Angulo-Jaramillo et al., 2000). In addition, near-saturated hydraulic
66 conductivities can be measured using a tension disk infiltrometer. The method is designed as a field
67 method, but has been occasionally applied in the laboratory. Using a tension disk infiltrometer, hydraulic
68 conductivities at supply tensions between ca. 0.5 and ca. 60 to 150 mm can be obtained, depending on
69 the specifications of the infiltrometer. All measurement techniques for saturated and near-saturated
70 hydraulic conductivity are laborious, time-consuming and constrained to a relatively small soil volume.

71 It is necessary to develop pedotransfer functions to estimate soil hydraulic conductivities for large-scale
72 modelling applications, as we cannot measure everywhere (Bouma, 1988; Van Looy et al., 2017;
73 Wösten et al., 2001). The development of a pedotransfer function requires a database from which it can
74 be derived. For example, the well-known pedotransfer function ROSETTA (Schaap et al., 2000) is
75 based on the open UNSODA database (Nemes et al., 2001). The equations published in Tóth et al.,
76 2015 are derived from the proprietary EU-HYDI database (Weynants et al., 2013). The pedotransfer
77 functions of Jarvis et al. (2013) are based on an unpublished meta-database containing tension-disk
78 infiltrometer data. Collecting published measurements of saturated and near-saturated hydraulic
79 conductivity measurements into meta-databases and pairing them with other existing databases is



80 essential to develop pedotransfer functions. A notable example is the SWIG database (Rahmati et al.,
81 2018) that collates more than 5000 datasets from soil infiltration measurements, covering the entire
82 globe. Another big effort in collecting information on saturated hydraulic conductivity is the newly
83 published SoilKsatDB (Gupta et al., 2021a), which combines saturated hydraulic conductivity data from
84 several large databases, amongst others UNSODA and SWIG, together with additional measurements
85 published in independent scientific studies. However, none of the databases cited above provide open-
86 access infiltration measurements at tensions near-saturation ($h > 0$ mm), which limits their use to the
87 estimation of saturated hydraulic conductivity.

88 Pedotransfer functions for saturated hydraulic conductivity exhibit rather poor predictive performance
89 with coefficients of determination R^2 not exceeding 0.25. (Weynants et al., 2009; Jorda et al., 2015).
90 Early approaches, like HYPRES (Wösten et al., 1999) and ROSETTA, focused solely on soil properties
91 like texture, bulk density and organic carbon content. At the time, it was not sufficiently recognized that
92 soil K_s is mostly determined by the morphology of macropore networks, especially in finer-textured soils
93 (Vereecken et al., 2010; Koestel et al., 2018; Schlüter et al., 2020). A pedotransfer function for K_s
94 requires therefore ideally a database that contains direct information on the macropore network itself.
95 But since such measures are even more cumbersome and time-consuming to obtain (e.g. by X-ray
96 tomography) than measuring hydraulic conductivity itself, it is more reasonable and makes more sense
97 to use proxies from which the macrostructure in a soil can be inferred. Ideal candidates would be root
98 growth and the activity of soil macrofauna, which both strongly determine the development of
99 macropore networks in soil (Meurer et al., 2020). However, they are difficult to measure. Proxies that
100 are more promising are land use and farming practises, such as tillage or soil compaction due to
101 trafficking. Plant growth and soil macrofauna in turn are influenced by the local climate. The climate
102 also sets boundaries for the land use and the associated soil management practices, and thus provides
103 feedback to root growth and macro-faunal activity. Wetting and drying cycles and thus the formation
104 and closure of cracks also are regulated by the climate as is splash erosion and soil crusting. It is
105 therefore not surprising that climate variables typically are correlated with saturated and near-saturated
106 hydraulic conductivities (Jarvis et al., 2013; Jorda et al., 2015; Hirmas et al., 2018; Gupta et al., 2021b).



107 Jorda et al., 2015 found that land use itself was the most important predictor for saturated hydraulic
108 conductivity.

109 The time of measurement of the hydraulic conductivity (or soil sampling) also has a crucial impact. In
110 an agricultural soil, the hydraulic properties of a freshly prepared seedbed differ from those measured
111 later at harvest. Several studies have demonstrated the evolution of hydraulic conductivity with time
112 (Messing & Jarvis, 1990; Messing and Jarvis, 1993; Bodner et al., 2013; Sandin et al., 2017). Soil
113 management options (such as tillage or the use of cover crops) actively influence the soil saturated and
114 near-saturated hydraulic conductivity. Information on their impact is therefore especially important, but
115 so far has hardly been investigated in meta-studies.

116 In this study, we quantified the effect of soil management practices on soil saturated and near-saturated
117 hydraulic conductivity, K_r . We also compared the strengths of relationships between K_r and soil
118 management practices and other potentially important influencing factors like soil properties, local
119 climate and details of the measurement methods. In this process, we expanded and published the
120 previously unpublished meta-database on tension-disk infiltration measurements that was first reported
121 by Jarvis et al. (2013). We referred to this database as OTIM in the following (Open Tension-disk
122 Infiltrometer Meta-Database). It complements the currently available public databases on hydraulic
123 conductivities, which are strongly based on laboratory measurements or ring infiltrometer methods.

124 2 Material and Methods

125 2.1 Meta-Database, OTIM

126 2.1.1 Data collection

127 The first version of OTIM was compiled for the study by Jarvis et al., 2013. The original database
128 contained 753 tension-disk infiltrometer data entries collated from 124 source publications, covering
129 144 different locations around the globe. We have extended this database by 544 new tension-disk
130 infiltrometer data entries from 48 additional studies that had been published after 2012. The search for
131 publications was carried out between 2021-05-31 and 2021-06-23 using the queries and search engines
132 detailed in Table A1.



133 We found 115 publications containing tension-disk infiltrometer measurements published in 2013 or
 134 later. We retained the data for further analysis when (i) K_h or the infiltration rate was measured at more
 135 than two tensions larger or equal to 5 mm and (ii) sufficient meta-data on soil and site properties (at
 136 least soil texture) as well as soil management practices (at least land use and tillage) were available. If
 137 a publication only reported infiltration rates, we calculated hydraulic conductivity using the method of
 138 Ankeny et al. (1991). Only 45 of the 115 publications fulfilled the above-mentioned criteria. Table A2
 139 summarises how many papers were rejected and for which reasons. For 27 of the 45 retained studies,
 140 we digitised the published K_h values from figures using WebPlotDigitizer (open-source web-based
 141 software created by Ankit Rohatgi, <https://automeris.io/WebPlotDigitizer/>). For cases in which K_h
 142 measurements were mentioned in a publication, but the results were not reported, we contacted the
 143 corresponding authors. We received the data in this fashion for three of these publications (Alletto et
 144 al., 2015; Larsbo et al., 2016a; Meshgi & Chui, 2013). The new studies containing data added to the
 145 OTIM database are summarised in Table 1.

146 **Table 1: List of new entries added to the Jarvis et al., 2013 database.**

| Reference | Land use | Tillage | Compaction | Sampling time | Data entries |
|-----------------------------|--------------------|-----------------------------------|---------------------------|-----------------------------|--------------|
| Alagna et al., 2015 | grassland | no tillage | not compacted | consolidated soil | 1 |
| Alletto et al., 2015 | arable | conventional tillage | unknown | consolidated soil | 60 |
| Bagarello et al., 2014 | arable | no tillage conventional tillage | unknown | unknown | 10 |
| Baranian Kabir et al., 2020 | grassland arable | no tillage | not compacted compacted | unknown consolidated soil | 4 |



| | | | | | |
|-------------------------|-----------|---|---------------------------------|---|----|
| Bát'ková et al., 2020 | arable | reduced tillage no tillage conventional tillage | unknown | consolidated soil soon after tillage | 12 |
| Bodner et al., 2013 | arable | no tillage | unknown | soon after tillage consolidated soil | 12 |
| Bottinelli et al., 2013 | arable | unknown conventional tillage reduced tillage no tillage | unknown | consolidated soil | 10 |
| Costa et al., 2015 | arable | conventional tillage reduced tillage no tillage | not compacted | consolidated soil | 3 |
| De Boever et al., 2016 | grassland | no tillage | not compacted | unknown | 6 |
| Tóth et al., 2014 | arable | conventional tillage | not compacted compacted | consolidated soil | 2 |
| Etana et al., 2013 | arable | conventional tillage | not compacted compacted | unknown | 2 |
| Fashi et al., 2018 | arable | no tillage reduced tillage conventional tillage | compacted not compacted | unknown | 8 |



| | | | | | |
|-------------------------|--|--|---------------------------------|----------------------|----|
| Fasinmirin et al., 2018 | arable woodland/plantation grassland | conventional tillage no tillage | not compacted compacted | unknown | 3 |
| Greenwood, 2016 | arable grassland | conventional tillage no tillage | unknown | consolidated soil | 4 |
| Hallam et al., 2020 | arable | conventional tillage | not compacted | unknown | 60 |
| Hardie et al., 2012 | arable | no tillage | not compacted | consolidated soil | 2 |
| Holden et al., 2014 | grassland | no tillage | not compacted | consolidated soil | 5 |
| Hyväluoma et al., 2019 | arable | conventional tillage | unknown | consolidated soil | 4 |
| Iovino et al., 2016 | arable grassland woodland/orchard | reduced tillage no tillage | unknown | consolidated soil | 3 |
| Kelishadi et al., 2013 | arable grassland | reduced tillage no tillage conventional tillage | not compacted | consolidated soil | 4 |
| Keskinen et al., 2019 | arable | no tillage conventional tillage | unknown | consolidated soil | 15 |



| | | | | | |
|-----------------------------|------------------------------|---|---------------------------|-----------------------------|----|
| Khetdan et al., 2017 | arable | no tillage | unknown | unknown | 4 |
| Larsbo et al., 2016a | arable | conventional tillage | not compacted compacted | consolidated soil unknown | 5 |
| Lopes et al., 2020 | woodland/orchard grassland | no tillage | not compacted | consolidated soil | 4 |
| Lozano et al., 2014 | arable | no tillage | not compacted | consolidated soil | 2 |
| Lozano-Baez et al., 2020 | grassland woodland/orchard | no tillage | not compacted | unknown | 18 |
| Matula et al., 2014 | grassland | no tillage | unknown | unknown | 3 |
| Miller et al., 2018 | arable | conventional tillage | unknown | consolidated soil | 10 |
| Mirzavand, 2016 | arable | conventional tillage reduced tillage no tillage | unknown | consolidated soil | 12 |
| Pulido Moncada et al., 2014 | arable grassland | conventional tillage no tillage | unknown | unknown | 4 |
| Rahbeh, 2019 | arable | conventional tillage | unknown | consolidated soil | 69 |



| | | | | | |
|----------------------------|------------------|-----------------------------------|---------------------------|--------------------------------------|----|
| Rienzner & Gandolfi, 2013 | arable | conventional tillage | not compacted | unknown consolidated soil | 18 |
| Sandin et al., 2017 | arable | conventional tillage | not compacted compacted | consolidated soil unknown | 7 |
| Soracco et al., 2015 | grassland | conventional tillage | not compacted compacted | unknown | 3 |
| Soracco et al., 2019 | arable | conventional tillage no tillage | unknown | consolidated soil | 6 |
| Wang, 2021 | arable | conventional tillage | unknown | soon after tillage consolidated soil | 25 |
| Wanniarachchi et al., 2019 | arable | conventional tillage | unknown | consolidated soil | 6 |
| Yu et al., 2013 | grassland | no tillage | unknown | unknown | 11 |
| Yusuf et al., 2017 | arable | no tillage | not compacted | consolidated soil | 1 |
| Yusuf et al., 2020 | arable | no tillage | not compacted | consolidated soil | 5 |
| Zeng et al., 2013 | woodland/orchard | conventional tillage | unknown | consolidated soil | 20 |



| | | | | | |
|--------------------|---------------------------------------|-----------------------------------|-------------------------|--|----|
| Zeng et al., 2012 | grassland | no tillage | unknown | consolidated soil | 6 |
| Zhang et al., 2013 | grassland arable | no tillage unknown | unknown | consolidated soil | 6 |
| Zhang et al., 2014 | arable | conventional tillage | unknown | consolidated soil | 4 |
| Zhang et al., 2016 | woodland/orchard arable | no tillage conventional tillage | unknown not compacted | consolidated soil soon after tillage | 24 |
| Zhang et al., 2021 | grassland woodland/orchard arable | no tillage conventional tillage | unknown | consolidated soil | 4 |
| Zhao et al., 2014 | arable grassland | conventional tillage no tillage | not compacted | unknown | 12 |
| Zhou et al., 2015 | arable grassland woodland/orchard | conventional tillage no tillage | not compacted | soon after tillage | 3 |

147

148 In addition to adding data from new publications to OTIM, we also revisited the studies contained in the
 149 original version of the database and collected additional information on soil management practices
 150 associated with the measured data. For each soil management option, OTIM contains two columns. In
 151 the first column, the information as given in the source publication is stored. The second column
 152 summarises this information into a few classes, which were subsequently used in the meta-analysis. In
 153 this study, we investigated effects of land use, tillage system, soil compaction and day of measurement



154 relative to the latest tillage operation on the field. A compaction class was assigned to a data entry only
155 if the plot had been described as 'compacted' or 'not compacted' in the source publication. 'Compacted'
156 data entries corresponded, for example, to infiltration measurements in wheel tracks or on plots of a
157 compaction experiment. The day of measurement relative to tillage was also included, with the data
158 labelled 'freshly tilled' when the authors in the source publication stated that the measurements had
159 taken place soon after tillage. Otherwise, it was assumed that the soil had already had time to
160 consolidate before the infiltration measurements were carried out. All soil texture data was mapped
161 onto the USDA classification system using the method proposed in Nemes et al. (2000).

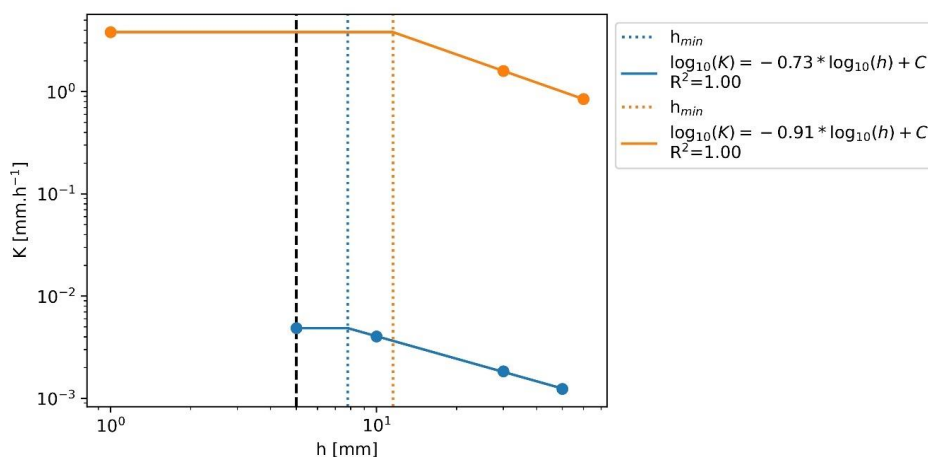
162 2.1.2. Climate data and soil classification

163 The climatic data entries provided in the database were created using the bioclimatic raster data
164 (BioClim) provided by WorldClim (worldclim.org). The data was averaged across the years 1970 to
165 2000 and had a 30 arc second resolution (~1 km²; Fick & Hijmans, 2017). The available climate
166 variables were mean annual temperature and precipitation, the mean temperature as well as mean
167 precipitation of the warmest, coldest, wettest and driest quarter and month, respectively, the
168 isothermality, the mean diurnal and annual temperature range, the seasonality for temperature and
169 precipitation. Besides the bio-climatic data in WorldClim we included the aridity index (here defined as
170 the annual precipitation divided by the potential evapotranspiration) as well as the average annual
171 potential evapotranspiration (ET₀). Both were inferred from the "Global Aridity Index and Potential
172 Evapotranspiration Climate Database v2" that is based on the WorldClim database (Trabucco & Zomer,
173 2019). The World Reference Base (WRB) soil type was also extracted from the source publications.
174 When it was not reported, the SoilGrids database by ISRIC (Poggio et al., 2021) was used to infer it.
175 The map contained information about the main soil type regarding the WRB classes (IUSS Working
176 Group WRB, 2015). The most probable soil type was chosen for each location. For all discussed climate
177 and soil maps, the python package "rasterio" (v1.2.10) was used to collect the variables from the
178 corresponding raster cell at the location coordinates given in the source publications.

179 2.1.3 Model fit to infer K_h at near-saturated tensions not measured



180 Tension-disk infiltrometers measure infiltration rates at a specific supply tension (Angulo-Jaramillo et
181 al., 2000). They consist of a ceramic disk to which a water reservoir and a bubbling tower is attached.
182 The ceramic disk is saturated and hydraulically connected to the soil by inserting a layer of fine sand
183 between the disk and the soil surface. The supply tension at the bottom of the ceramic disk is adjusted
184 by the bubbling tower. The measured unconfined (i.e. three-dimensional) infiltration rates are then
185 commonly converted to hydraulic conductivities with the aid of the Wooding equation (Wooding, 1968).
186 Note that unconfined tension-disk infiltrometers cannot provide measurements at a tension of zero, i.e.
187 K_s . Even if many publications report K_s values obtained from tension-disk infiltrometers, these
188 measurements must have been conducted at tensions slightly larger than zero, as water would
189 otherwise have freely leaked out of the tension disk. For this reason, we set the tensions for K_s
190 measurements to 1 mm, but still referred to these data as saturated hydraulic conductivity.



191

192 **Figure 1: Example of linear fit in log-space. K_s values were assigned a tension of 1 mm for**
193 **illustration purposes. The equations for the linear part of the fit are shown in the legend.**
194 **C represents the intercept with the y-axis of the linear fit in log-space, h_{min} corresponds to**
195 **the supply tension at which the largest pores in the soil are water-filled.**

196 Following Jarvis et al., 2013, we interpolated K_r for tensions in-between the ones measured in the
197 source publications. We achieved this by fitting a log-log linear model with a kink at a tension h_{min} , which
198 denotes the tension at which the largest effective pores in the soil are water-filled (see Figure 1).



199 Therefore, $K_h = K_s$ for all tensions $h \leq h_{min}$. If K_s was not measured but instead a K_h value at $h \leq 5$ mm
200 was available, K_s was set to the available K_h value (Figure 1 orange line). In cases where more than
201 one K_h value was measured at a tension smaller or equal to 5 mm (including $h = 0$ mm, i.e. K_s), we
202 averaged them and fixed K_s and K_h for $h \leq h_{min}$ to the average (Figure 1 green line). K_h values at $h > 5$
203 mm were used to fit the log-log linear relationship. The tension at which the fitted log-log slope
204 intersected with K_s defined h_{min} . We used the fitted model to estimate all K_h values for tensions for 10
205 $\leq h \leq 100$ mm at 10 mm intervals. The K_h values were only interpolated between the tensions that were
206 measured in the source publication. The only exceptions from this rule were made in the case where a
207 K_h value for a tension of 80 or 90 mm was provided together with at least one other K_h value measured
208 at a smaller tension. Then, the missing K_h values were extrapolated up to a tension of 100 mm. Figure
209 1 shows examples of model fits. Only entries with an R^2 greater or equal to 0.9 were retained in the
210 analysis.

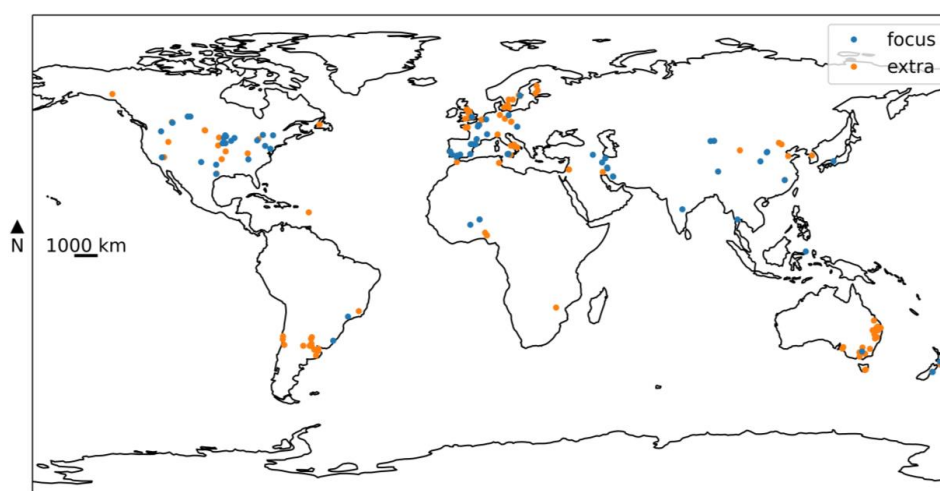
211 2.2 Data availability and spatial coverage

212 Although 92% of the OTIM data is from the topsoil, it also contains some data points measured at
213 greater soil depths. In the following meta-analysis, only measurements from the topsoil were included
214 to prevent bias and all datasets measured at soil depths below 200 mm were removed. Last but not
215 least, we found that the relationship between supply tension and K_h was distorted if data entries were
216 included that did not cover the complete tension range from $h = 0$ to 100 mm. Possible reasons for the
217 difficulties to match K_h data from tension series with different lengths are discussed at the beginning of
218 the results and discussion section. Otherwise, we focused on data entries that included K_h values for
219 the complete tension range in the exploratory data analysis and the meta-analyses. The available
220 datasets after these filtering steps correspond to the ones indicated in blue (and termed 'focus') in the
221 following figures.

222 Most tension-disk infiltrometer studies were conducted in Europe, North America and Southeast
223 Australia (Figure 2). Clearly, fewer studies have been carried out in Asia, South America and Africa.
224 The lack of datasets from Russia, Mesoamerica, the arctic regions and the tropics is remarkable. This
225 geographical bias is aggravated if only measurements on the topsoil are considered that allow



226 inferences about K_h for the complete range of tensions ($0 \leq h \leq 100$ mm) with a sufficiently good
227 coefficient of determination. Then, all the data entries collected in southern South America and south-
228 eastern Australia were omitted, as well. Overall, the data in OTIM mostly stem from temperate climate
229 regions.



230

231 **Figure 2: Map of the study locations collected in the OTIM. The values are shown for the**
232 **filtered entries ('focus') and in parenthesis for all the entries available in the database**
233 **('focus' and 'extra').**

234 Figure 3 depicts the number of K_h values available for $0 \leq h \leq 100$ mm. These figures represent the
235 hydraulic conductivities derived from the log-log linear model presented above, not the raw data
236 measured and reported in the source publications. A large number of entries span the full range of
237 tensions of interest (0 to 100 mm), whereas a smaller number of entries only have data up to a tension
238 of 60 mm. Often, but not always, such data series were obtained with the widely available Mini-Disk
239 infiltrometer distributed by the *Meter* group (formerly by *Decagon*), which is limited to tensions $h \leq 70$
240 mm. An overview on the metadata included in OTIM is given in Table 2. Data gaps are present,
241 especially for bulk density and for information on the soil management at the study site, apart from
242 tillage operations. Note that the annual mean temperature and precipitation are only two examples

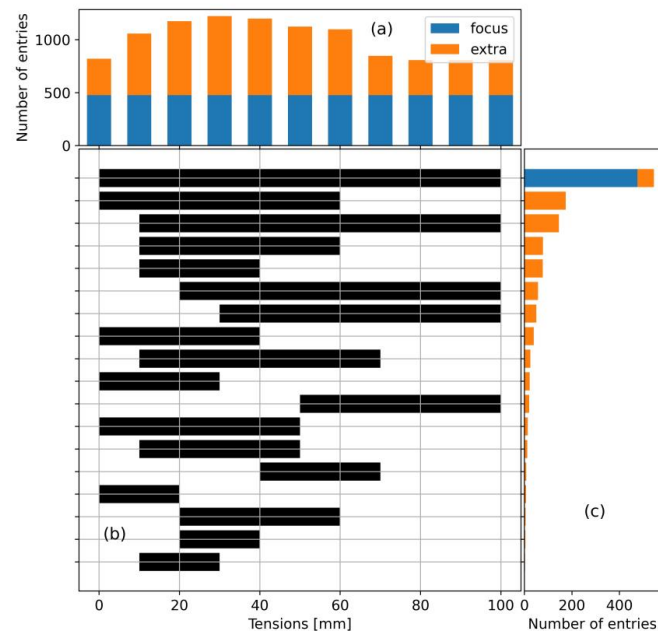


243 representing the climatic variables enumerated in section 2.3. There are very few missing values for
 244 the climate data, since it was estimated from the coordinates of the study sites. The same holds for the
 245 elevation data and information on the WRB soil type.

246 **Table 2: Number of entries and gaps for each feature along with units and range (if**
 247 **continuous) or choices (if categorical). The values are shown for the filtered entries**
 248 **(‘focus’) and in parenthesis for all the entries available in the database (‘focus’ and ‘extra’).**

| Type | Predictor | Unit | Range/Choices | Number of entries | Number of gaps |
|------------|--------------------------------|---------------------|---|-------------------|----------------|
| Soil | Sand content | kg kg ⁻¹ | 0.0 -> 0.9 (0.0 -> 1.0) | 402 (1070) | 64 (215) |
| Soil | Silt content | kg kg ⁻¹ | 0.0 -> 0.8 (0.0 -> 0.8) | 402 (1070) | 64 (215) |
| Soil | Clay content | kg kg ⁻¹ | 0.0 -> 0.7 (0.0 -> 0.8) | 405 (1107) | 61 (178) |
| Soil | Bulk density | g cm ⁻³ | 0.5 -> 1.8 (0.1 -> 2.2) | 324 (771) | 142 (514) |
| Soil | Soil organic carbon | kg kg ⁻¹ | 0.0 -> 0.1 (0.0 -> 1.0) | 339 (938) | 127 (347) |
| Climate | Annual mean temperature | °C | -0.4 -> 29.1 (-3.8 -> 29.1) | 466 (1214) | 0 (71) |
| Climate | Annual mean precipitation | mm | 22.0 -> 3183.0 (22.0 -> 3183.0) | 466 (1214) | 0 (71) |
| Climate | Average aridity index | - | 0.0 -> 1.9 (0.0 -> 2.8) | 466 (1214) | 0 (71) |
| Climate | Precipitation seasonality (CV) | - | 9.9 -> 138.5 (9.6 -> 138.5) | 466 (1214) | 0 (71) |
| Climate | Mean diurnal range | °C | 6.9 -> 18.2 (4.8 -> 18.5) | 466 (1214) | 0 (71) |
| Management | Land use | - | arable, bare, grassland, woodland/plantation | 453 (1249) | 13 (36) |
| Management | Tillage | - | conventional tillage, no tillage, reduced tillage | 422 (1190) | 44 (95) |
| Management | Soil compaction | - | compacted, not compacted | 76 (265) | 390 (1020) |
| Management | Sampling time | - | soon after tillage, consolidated soil | 367 (993) | 99 (292) |

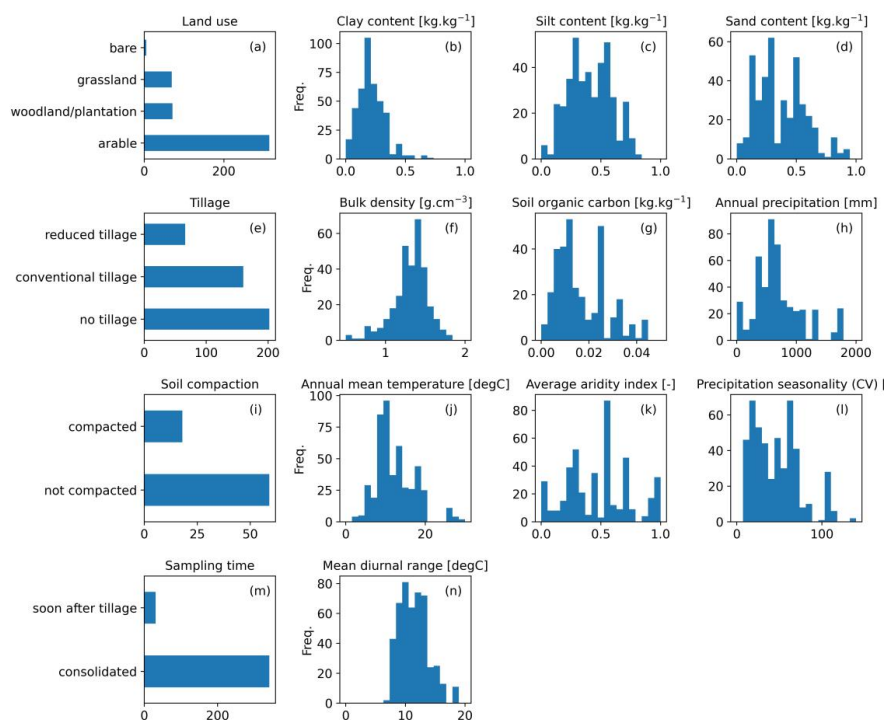
249



250

251 **Figure 3: (a) number of available K_t values per supply tension, (b) range of available**
252 **tensions and (c) their respective occurrence in the database. The values are shown for the**
253 **filtered entries ('focus') and in parenthesis for all the entries available in the database**
254 **('focus' and 'extra').**

255 The metadata for the datasets used in the exploratory data analysis are summarized in Figure 4. OTIM
256 contains predominantly data from arable fields. The distributions of the climate variables confirms that
257 the data in OTIM was also mostly acquired in temperate climates, with a bias towards the somewhat
258 drier climates that are most typical for arable land. The soil texture, bulk density and organic carbon
259 content data also appear reasonably representative for soils in this climate zone.



260

261 **Figure 4: Distributions of continuous and categorical variables in the 'focus' dataset.**

262 2.3 Exploratory data analysis

263 Some source publications only provided a few data entries for K_h , sometimes only comparing two
264 different treatments, while other source studies contain data for a larger number of treatments and/or
265 sites. In some publications, data for all individual tension-disk measurements are available, even if
266 replicates were measured. In others, only averages of the replicated measurements are reported, while
267 still others yield average K_h values for individual replicated treatment blocks. This makes appropriate
268 data weighting complicated, but also extremely important when analysing the meta-dataset. It also
269 introduces uncertainty, because it is not always clear whether the replicated averages were calculated
270 using the geometric or the arithmetic mean. Considering that hydraulic conductivities at or near
271 saturation are known to be log-normally distributed, the former would be best. In the following, we



272 assumed that geometric averaging was used when replicated values were reported in source
273 publications. In the following, we calculated data weights as

$$274 \quad \omega_i = \frac{n_{r,i}}{\sqrt{N_i}} \quad \text{Equation 1}$$

275 where ω_i is the weight for data entry i , $n_{r,i}$ is the number of replicates from which the values of i were
276 averaged and N_i is the total number of measurements included in the publication from which data entry
277 i was obtained. With this approach, we up-weighted data entries according to the number of replicate
278 measurements from which they were averaged and down-weighted the impact of studies that published
279 larger amounts of data.

280 We used weighted Spearman rank correlation coefficients to investigate relationships between
281 continuous variables. We considered correlations significant if they exhibited p-values of less than 0.05.
282 The latter were determined numerically by running randomization tests with 200 repetitions.

283 2.4 Meta-analysis

284 Data entries in OTIM with specific land use or management were very unevenly distributed. For
285 example, the large majority of data was measured on sites with land use 'arable' (see Figure 4a). Such
286 uneven distributions may lead to bias when averaged over all entries of a specific feature in exploratory
287 data analyses. We therefore investigated the effects of land use and management as well as soil
288 compaction and time of measurement on K_r with the aid of pairwise comparisons published within
289 individual studies and calculated effect sizes (ES) for each investigated class.

290 To reduce bias arising from the varying number of data entries published within individual studies, we
291 grouped all entries according to the factors land use, tillage, compaction, and sampling time. Here we
292 only considered binary pairs, that is arable or not arable in the case of land use and tilled or not tilled,
293 compacted or not compacted as well as 'measured soon after tillage' or 'measured on consolidated soil'
294 for the other three factors. In addition, we checked whether different entries within individual studies
295 stemmed from the same or a very similar site. We did this by comparing the respective USDA texture
296 classes and a climate variable, namely the aridity class. All data entries within each individual study that



297 exhibited identical land use, soil management, soil compaction, sampling time, texture and aridity were
298 averaged and the number of corresponding replicates was summed.

299 For each binarized factor (e.g. tillage), a *control* value was chosen (e.g. zero tillage). All values different
300 from the control represent the *treatment* (e.g. conventional tillage and reduced tillage). Within individual
301 studies, pairs among the averaged entries were formed for each combination of a control and a
302 treatment value. These pairs were used to compute the effect size. Following Basche & DeLonge
303 (2019), we defined the effect sizes as the log₁₀ of the ratio of $K_{h,t}$ of the treatment divided by $K_{h,c}$ of the
304 control

$$305 \quad ES_l = \log_{10} \left(\frac{K_{h,t}}{K_{h,c}} \right) \quad \text{Equation 2}$$

306 where the subscript l indicates the l^{th} pair for which the effect size was computed and the indices ' t ' and
307 ' c ' stand for treatment and control, respectively. The average effect size ES for each of the four
308 investigated factors was calculated as the weighted mean of the individual ES_l using the weight

$$309 \quad W_l = \frac{v_c v_t}{v_c + v_t} \quad \text{Equation 3}$$

310 where the subscript l indicates again the l^{th} pair for which the effect size was computed and v_c and v_t
311 denote the number of (summed) replicates for control and treatment, respectively. In addition, we
312 calculated the weighted standard error

$$313 \quad \sigma_{\overline{ES}} = \sqrt{\frac{\sum_{l=0}^n w_l (ES_l - \overline{ES})^2}{\frac{n-1}{n} \sum_{l=0}^n w_l}} \quad \text{Equation 4}$$

314 where \overline{ES} is the mean effect size. Table 3 summarises the evaluated factors, the number of pairs
315 involved and the number of different studies from which the pairs were obtained.

316 To estimate the robustness of the effect size, we carried out a sensitivity analysis using the Jackknife
317 technique, similarly to Basche & DeLonge, 2019. This method aims to show the sensitivity of the



318 averaged effect size to data from specific studies. For each factor, a given number of studies was
319 randomly picked and removed from the dataset. The averaged effect size and its standard error was
320 computed with the rest of the dataset. The process started by removing one study, after which up to
321 nine more studies were removed. This random selection was repeated 50 times to rule out bias. The
322 average of the means and standard errors for the 50 realisations was computed and plotted. Observed
323 effect sizes were judged trustworthy if they did not change after removal of studies to calculate
324 them. We constrained the sensitivity analyses in our study to the effect sizes for K_s and K_{100} .

325 **Table 3: Number of studies and paired comparison with their respective control and**
326 **treatment values used for the meta-analysis exemplary for the K_{100} values.**

| Factor | Control | Treatments | Studies | Paired comparisons |
|---------------|-------------------|---------------------------------------|---------|--------------------|
| Land use | not arable | arable | 10 | 24 |
| Tillage | no tillage | conventional tillage, reduced tillage | 15 | 32 |
| Compaction | not compacted | compacted | 6 | 8 |
| Sampling Time | consolidated soil | soon after tillage | 6 | 12 |

327

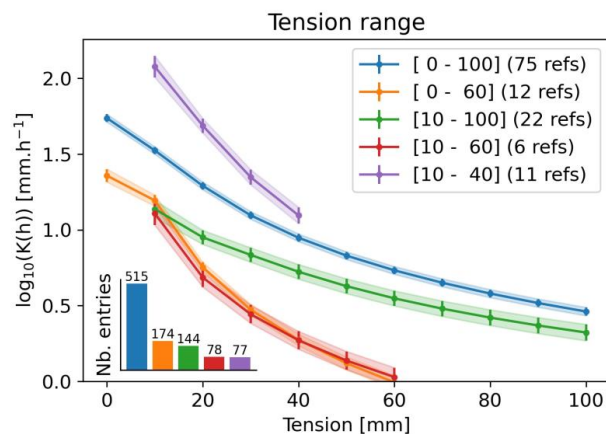
328 3 Results and discussion

329 3.1 Differences between data entries with different tension ranges

330 If all data are considered ('focus' and 'extra'), Figure 3 illustrates that approximately 40% of the data in
331 OTIM provided K_h for every h with $0 \leq h \leq 100$ mm. For another 40%, K_h was only measured in the wet
332 range, i.e. at tensions below 70 mm. The remaining K_h data was only acquired at the dry range. Here,
333 we counted all data entries for which K_s were not measured and could not be estimated. Figure 5 shows



334 how data from entries with complete, dry and wet ranges differed. The K_h for the wet range receded
335 faster with increasing tension than series that also included measurement in the dry range. A large
336 portion of these datasets were obtained with the Mini-Disk infiltrometer. However, a closer inspection
337 of the impact of the disk diameters used to acquire the respective K_h did not confirm suspicions that the
338 bias was related to the use of this special type of infiltrometer (see Figure 6a). The observed differences
339 between the K_h curves could have been introduced by co-correlations with soil texture or climate.
340 Another explanation may be experimenter bias, since individual research groups tend to use specific
341 tension ranges for more than one study. In this study, however, we focused solely on data entries for
342 which we were able to reconstruct K_h for all h in between 0 and 100 mm supply tension in the following
343 exploratory data analyses and meta-analyses. This greatly facilitated the data interpretation.



344

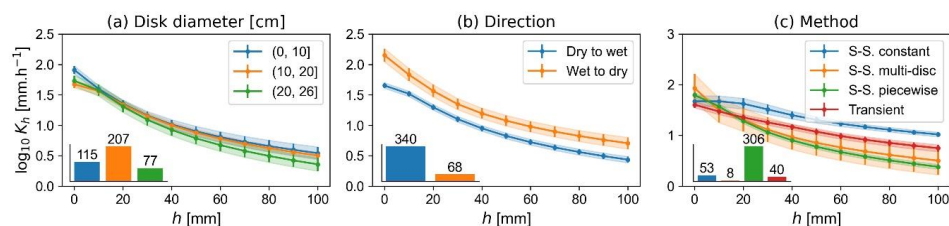
345 **Figure 5: Evolution of weighted mean K_h with tension available in OTIM, sorted by the**
346 **tension range the data was spanning. The number of publications from which the data**
347 **originated is shown between parentheses in the legend. The shaded areas and the error**
348 **bars represent the weighted standard error of the mean.**

349 3.2 Statistical relationships between K_h and methods used

350 Figure 6a confirms that the diameter of the tension disk did not have a systematic impact on the results.
351 The majority of the data were collected starting under dry conditions (large tensions) and subsequently
352 measured under increasingly wet conditions (smaller tensions). Figure 6b illustrates that beginning the
353 experiment under wet conditions is associated with larger hydraulic conductivities at identical supply



354 tensions. This is well known and is referred to as hysteresis, which is due to ink-bottle effects, impacts
 355 of water repellency, air entrapment and swelling of clay particles (Hillel, 2004). Figure 6c shows that the
 356 large majority of studies used the ‘steady-state piecewise’ method to solve the Wooding equation and
 357 convert the measured infiltration rates to hydraulic conductivities. This method leads to smaller K_h for
 358 larger tensions than the other methods. The ‘transient’ and ‘steady-state constant’ methods yielded
 359 larger K_h in the unsaturated range. For the latter method, it is known that it overestimates unsaturated
 360 K_h (Jarvis et al., 2013). We tested whether excluding data from ‘transient’ and ‘steady-state constant’
 361 methods changed the results of the meta-analyses, but found that they only changed to a minor degree.
 362 Data from all methods were therefore included in the following. Note that the ‘transient’ method was
 363 mostly applied in conjunction with Mini-Disk Infiltrometers, albeit the respective data is not included in
 364 Figure 6 since it does not span the entire suction range.



365

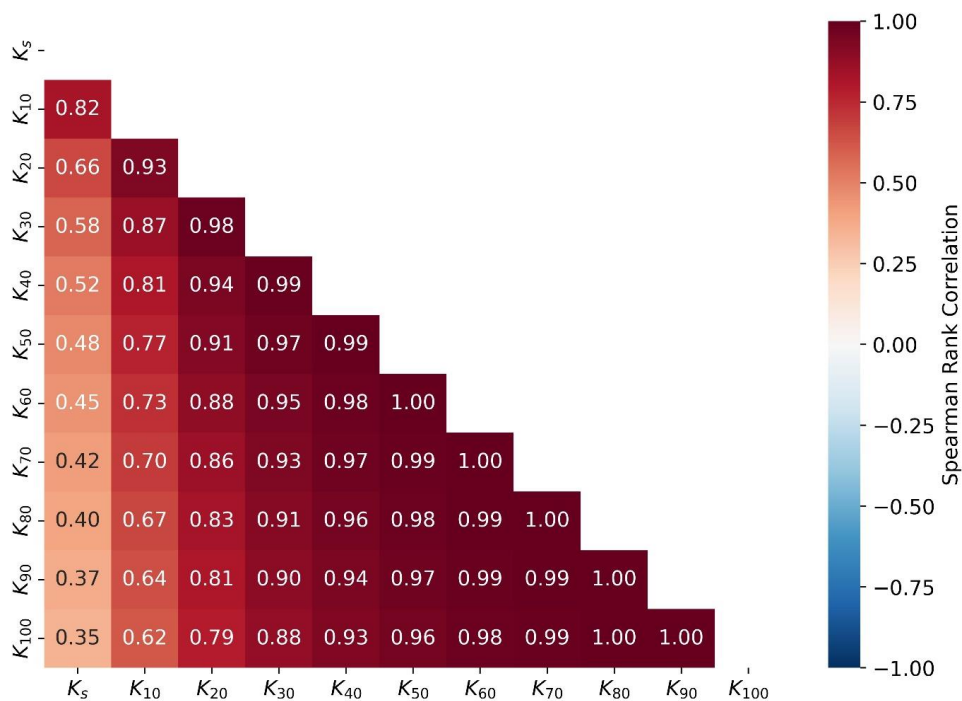
366 **Figure 6: Evolution of weighted mean K_h as a function of applied tension for (a) disk**
 367 **diameter, (b) direction and (c) method of fitting. ‘S-S.’ stands for ‘steady-state’. More**
 368 **specifically, the method ‘S-S. constant’ is outlined in Logsdon and Jaynes (1993), ‘S-S.**
 369 **multi-disc’ in Smettem and Clothier (1989), and ‘S-S. piece-wise’ in Reynolds and Elrick**
 370 **(1991) or Ankeny et al. (1991) and ‘Transient’ in Zhang (1997) or Vandervaere et al. (2000).**
 371 **The shaded areas and the error bars represent the weighted standard error of the**
 372 **mean. The bar plots in each subplot indicate how many data points of each class were in**
 373 **the data set.**

374 3.3 Correlation between K_h at different tensions

375 The fact that correlations between K_h estimated at supply tensions between 40 and 100 mm were
 376 relatively stable (Table 4) indicates that the respective flow paths and/or mechanisms remained very
 377 similar in this tension range. However, these correlations weakened at tensions between 10 and 20
 378 mm, giving rise to the existence of a threshold above which water flow in the largest macropores
 379 becomes the dominant flow mechanism. The poor correlation between K_s and K_h at larger supply



380 tensions is in line with findings that K_s is not well suited to infer to soil unsaturated hydraulic
 381 conductivities (Schaap and Leij, 2000).



382

383 **Table 4: Weighted Spearman rank correlation coefficients between K_h at different tensions.**

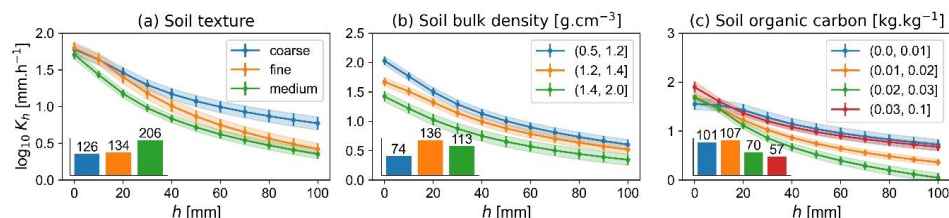
384 **Correlation coefficients are shown up to p-values of 0.001.**

385 3.4 Statistical relationships between K_h and soil properties

386 Soils with coarse texture exhibited larger K_h in the unsaturated range, which is caused by the large and
 387 abundant primary pores in between individual sand grains (Figure 7a). At saturation, the average
 388 hydraulic conductivity of all three texture classes was similar. This is explained by the presence of large
 389 structural pores in the medium and fine-textured soils. Medium-textured soils had the lowest K_h in the
 390 investigated range of tensions, which may be due to a denser soil matrix in loamy soils and a lower

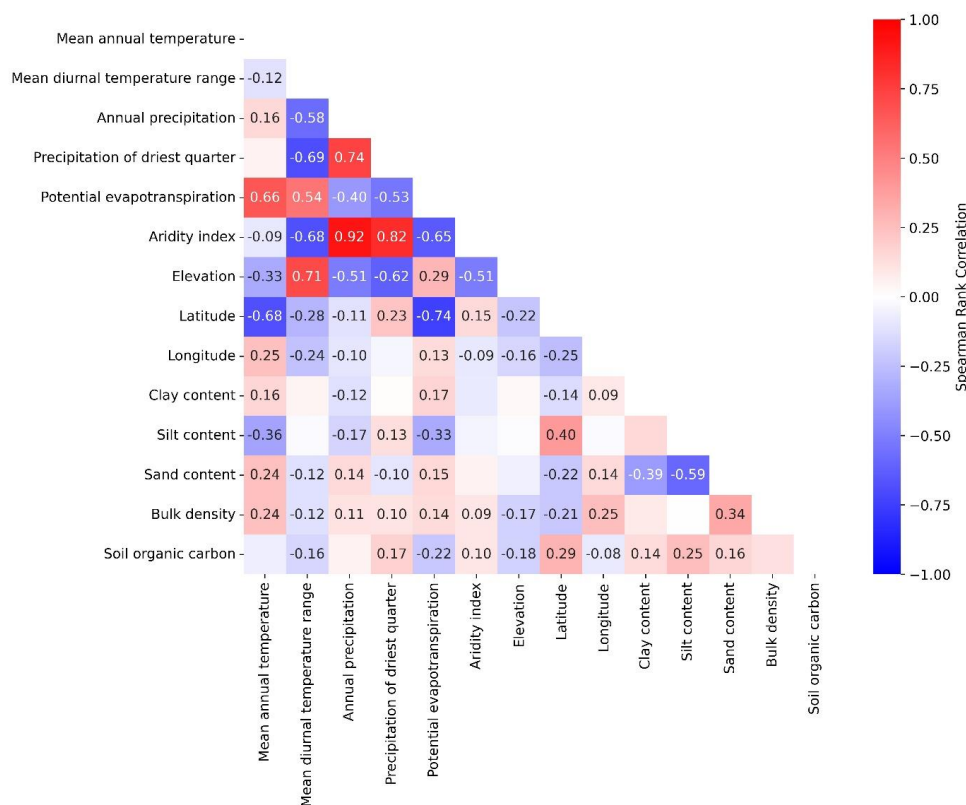


391 structural stability of silty soils. Larger bulk densities decreased K_h across the whole range of
392 investigated tensions, which reflects the reduced porosity with increasing bulk density (Figure 7b).
393 The hydraulic conductivity in the saturated and near-saturated range is especially affected by soil
394 compaction, which predominantly reduces the abundance and connectivity of macropores (Pagliai et
395 al., 2004; Whalley et al., 1995). Large bulk densities are also known to reduce burrowing activities of
396 the soil macrofauna (Capowiez et al., 2021) as well as root growth (Lipiec & Hatano, 2003), also leading
397 to less abundant and less connected large macropores. An increase in the soil organic carbon content
398 was connected with smaller K_h at the dry end of the investigated tension range if soils with organic
399 carbon contents of more than 0.03 kg.kg⁻¹ were excluded (Figure 7c). This decrease may be explained
400 by water repellency, which is generally positively correlated with organic carbon content. A similar
401 observation was already reported in Jarvis et al., 2013. Note that no major correlations of SOC with soil
402 texture were observed in the investigated dataset (Table 5). For soils with organic carbon contents
403 larger than 0.03 kg.kg⁻¹, K_h increased once again. This may indicate that, above this threshold, better-
404 developed macropore networks associated with large SOC contents (e.g. Larsbo et al., 2016b)
405 outweighed any effects of water repellency.



406

407 **Figure 7: Evolution of weighted mean K_h as a function of applied tension for (a) soil texture,**
408 **(b) soil bulk density and (c) soil organic carbon. The shaded areas and the error bars**
409 **represent the weighted standard error of the mean. The soil textures were classified using**
410 **USDA texture classes as follows: fine (clay, clay loam, silty clay, silty clay loam), medium**
411 **(silt loam, loam), coarse (loamy sand, sand, sandy clay, sandy clay loam, sandy loam). The**
412 **bar plots in each subplot indicate how many data points of each class were in the data set.**



413

414 **Table 5: Weighted Spearman rank correlation coefficients between climate variables,**
 415 **elevation above sea level and soil properties. Correlation coefficients are shown up to p-**
 416 **values of 0.001.**

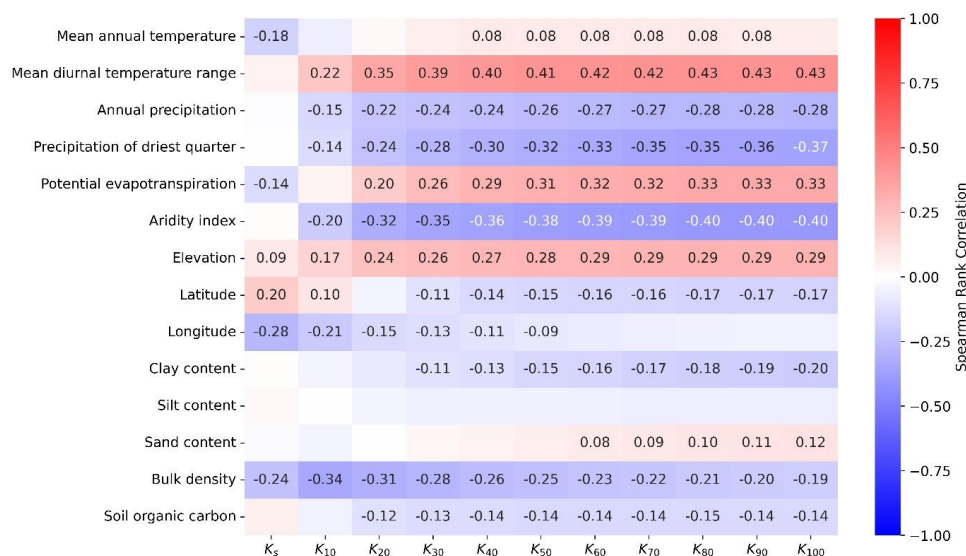
417 **3.5 Statistical relationships between K_h and climate variables**

418 One important observation made in recent years was that saturated and near-saturated hydraulic
 419 conductivities correlated strongly with climate variables (Jarvis et al., 2013; Jorda et al., 2015; Hirmas
 420 et al., 2018). Table 6 gives an overview of weighted Spearman rank correlations between K_h and six of
 421 the 20 climate variables included in OTIM that exhibited the strongest correlations with K_h . The elevation
 422 of the sampling site above sea level, its latitude and longitude, soil texture, bulk density and soil organic
 423 carbon content are also shown for comparison. It is striking that the soil properties were less well
 424 correlated with K_h than some of the climate variables. Of the three USDA texture fractions, the clay
 425 content was negatively and the sand content positively correlated with K_h at the drier investigated



426 tension range, while no significant correlations were found for the silt fraction (Table 6). Only the bulk
 427 density exhibited correlation coefficients as large as the climate variables.

428 The largest absolute values of the weighted rank correlations were observed for the mean diurnal range
 429 of temperature and the aridity index. Both reach a maximum at the dry end of the considered tension
 430 range, i.e. for K_{100} , with correlation coefficients of 0.43 and -0.4, respectively. Table 5 reveals that both
 431 of these best correlated climate variables were accidentally correlated with choices in experimental
 432 design and data evaluation made by the investigators in the respective source studies that will amplify
 433 these observed correlations to K_h . However, if a smaller dataset is considered in which such
 434 methodological bias as well as potential bias due to differences in land use were eliminated, the
 435 correlations persisted (Table B1). We therefore infer that the observed effect of climate on K_h is real.



436

437 **Table 6: Weighted Spearman rank correlation coefficients between K_h at different tensions**
 438 **and climatic features and soil properties. Correlation coefficients are shown up to p-values**
 439 **of 0.001.**



440 The annual mean diurnal temperature range and the aridity index were strongly correlated with each
441 other, with a weighted correlation coefficient of -0.68 (Table 5). Strong correlations to at least one of
442 these two variables with absolute values >0.6 were also found for most of the investigated climate
443 variables. It is therefore difficult to separate the climate effects due to these strong inter-correlations.
444 Nevertheless, it is striking that the mean annual diurnal temperature ranges are much better correlated
445 with K_{100} than the mean annual temperature itself (Table 6). In addition, the mean annual precipitation
446 in the driest quarter of the year and the precipitation in the driest quarter of the year exhibited stronger
447 correlations than the mean annual precipitation. It appears that temperature and precipitation
448 fluctuations are more strongly coupled to near-saturated hydraulic conductivities than the absolute
449 temperatures or precipitation amounts.

450 Among possible reasons for the observed correlations may be increased splash erosion during heavy
451 rainfalls that are common in regions with large precipitation seasonality, more soil compaction in wetter
452 climates due to trafficking, a larger vertical burrowing activity of soil fauna in climates with large diurnal
453 temperature ranges, more vertically oriented root systems in arid climates or climate specific choices in
454 land use and soil management. The data in OTIM cannot provide an answer to these questions.
455 Investigations of such relationships should be the focus of future studies.

456 Another site factor that is positively correlated with K_r is the elevation above sea level (Table 6). Notably,
457 elevation above sea level also was found to be an important predictor for K_s in Gupta et al. (2021b),
458 which suggests that there are indeed pedogenetic reasons behind the observed correlation. In the case
459 of infiltrometer measurements, the decreased atmospheric pressure with height on the supply tension
460 can be neglected. The supply tension is always equivalent to the weight of the water column adjusted
461 in the bubbling tower. The weight of the water column will be smaller due to the general decrease of
462 earth's gravitational constant with height due to a larger centrifugal force. However, the weight of the
463 water column would only be reduced by approximately one or two percent. Also, indirect influences of
464 larger heights on the infiltration rate cannot explain the observed correlation. A lower temperature would
465 make the water column denser. However, the effect would be less than 1% in the relevant temperature
466 range. In contrast, a lower temperature would increase the viscosity of water to a much larger degree,



467 e.g. by up to approximately 30% between temperatures of 10 and 20 °C. The temperature effect should
468 thus lead to a negative correlation between elevation and K_h , which is the opposite of what was
469 observed. Bias in the K_h measurements due to such physical effects can thus be ruled out. Elevation
470 may instead be a proxy for well-drained soils, as stagnant soil water and high groundwater tables are
471 less likely with height above sea level. This may favour soil life and better developed root systems and
472 decrease risks of compaction when the soil is trafficked.

473 The observed correlations of K_h with latitude and longitude probably reflect co-correlations with climate
474 variables together with experimenter bias, since it appears likely that approaches in setting up tension
475 disk infiltrometers systematically vary between continents, e.g. America and Europe.

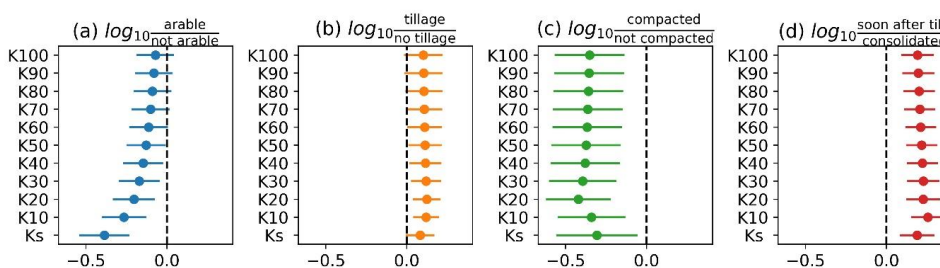
476 Bulk density was the only soil property that exhibited (negative) correlation strength of > 0.3 to any K_h ,
477 (Table 6). The underlying reasons have been discussed above. Notably, the strongest correlations were
478 found at and very close to saturation, probably due to the detrimental effect of soil compaction on
479 macroporosity and macropore connectivity. The more compaction, the less macroporosity remains and
480 the higher the bulk density, which in turn decreases root growth and bioturbation (Capowiez et al., 2021;
481 Lipiec and Hatano, 2003). The only pedo-climatic factor with relatively larger correlation strength (-0.31)
482 with the saturated hydraulic conductivity was the bulk density (Table 6).

483 3.6 Effects of land use, tillage, compaction and sampling time

484 The average \log_{10} response ratios shown in Figure 8 illustrate the effects of land use and soil
485 management on K_h for $0 \leq h \leq 100$ mm. Note that a value of ± 0.3 in the \log_{10} response ratio corresponds
486 to a factor 2. Hence, K_s for uncompacted soil was found to be approximately twice as large as for
487 compacted soil (see Figure 8c). Arable land exhibited clearly smaller K_s than grasslands and forests,
488 which is in line with observations made by Basche & DeLonge, 2019. This difference became smaller
489 with higher tensions (Figure 8a). The large difference in K_h close to saturation was likely related to traffic
490 compaction as well as tillage operations that were applied to the majority of the investigated arable
491 soils, which lead to the destruction of connected biopores and hence a reduced K_s . On the other hand,
492 tillage breaks up intact soil into individual soil aggregates, which creates, at least initially, a well-
493 connected network of inter-aggregate pores that increase K_h in the near-saturated range (Sandin et al.,



494 2017; Schlüter et al., 2020). This effect of tillage can explain why near-saturated K_h under conventional
 495 and reduced tillage was larger than under no-till (Figure 8b). However, in this case, even K_s was larger
 496 in the tilled fields. It is likely that K_s was reduced in the no-till treatments due to traffic compaction on
 497 the fields and a lack of soil loosening by tillage as compared to conventionally tilled treatments. Note
 498 however, that we only investigated topsoils in this study. It is not clear that how different tillage types
 499 affect K_h in the subsoil. The impact of soil compaction on K_h was clearly negative in the entire
 500 investigated range of tensions (Figure 8c), which is explained by the reduction of porosity, and
 501 especially the macroporosity during compaction (see also Figure 7b). In contrast, if the K_h
 502 measurements were carried out shortly after tillage operations, K_h was increased for all investigated
 503 tensions, especially very close to saturation (Figure 8d). This confirms that tillage initially increases K_s ,
 504 but that subsequent soil consolidation preferentially disconnects the largest macropores. As a
 505 consequence, K_h at and very close to saturation is reduced more strongly than K_h for higher tensions.



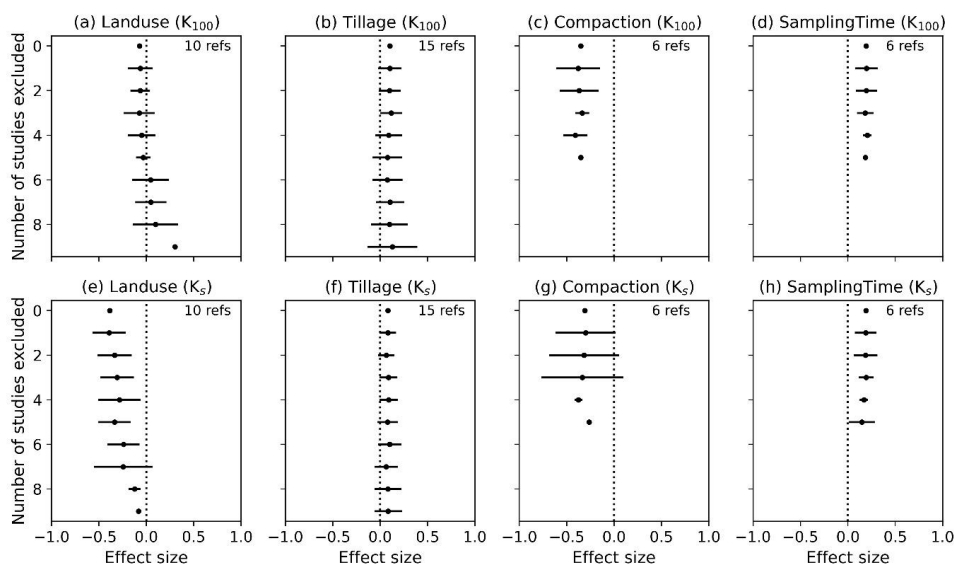
506

507 **Figure 8: Weighted mean \log_{10} response ratio (effect size) of K_h for from K_{100} to K_s for**
 508 **different management practises where the controls were ‘not arable’, ‘no tillage’, ‘no**
 509 **compaction’ and ‘consolidated soil’ respectively. Positive effect size means that the value**
 510 **of the treatment is greater than the control. Dashed line shows the “no effect” (no**
 511 **difference between treatment and control). Error bars represent the weighted standard**
 512 **error of the mean.**

513 Figure 9 shows the results of the sensitivity analyses for the effect sizes depicted in Figure 8. The effect
 514 of land use for K_{100} turned out to be the most sensitive to the removal of studies (Figure 9a). The
 515 direction of the effect even changed after removal of six studies, indicating that higher K_{100} for arable
 516 compared to non-arable fields were not just occasional observations but occurred more frequently. More
 517 studies would be needed to properly characterise the effect of land use on K_{100} . The remaining



518 sensitivity analyses for all the other factors showed that removal of studies did not change or destabilise
519 the results for both K_{100} and K_S .

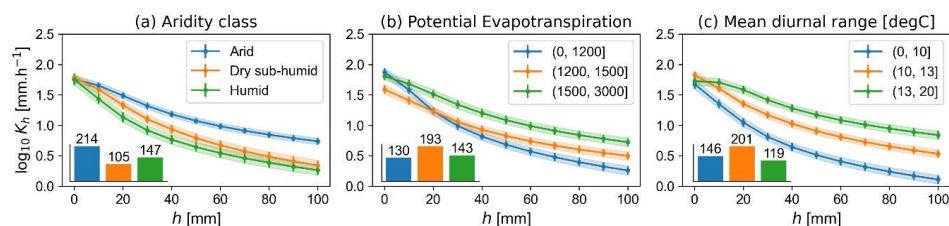


520

521 **Figure 9: Sensitivity analysis of the weighted effect size of K at 100 mm tension and K_S for**
522 **the management practice investigated using the Jackknife technique. The error bars**
523 **represent the standard error.**

524 3.7 Comparison of effect size of land use and management and sampling time with 525 effect of climate and soil properties

526 Effect sizes could only be computed for land use and management, compaction as well as sampling
527 time. It is therefore difficult to relate the impact of these factors to the ones of measurement method,
528 climate variables and soil properties. Comparisons between figures 6, 7 and 10, on the one hand, with
529 Figure 8 provide some insight. Land use and management related effects and sampling time (Figure 8)
530 seem to have a similar effect on K_h , as soil properties (Figure 7) and measurement method (Figure 6).
531 Climate variables seem to have a larger impact on K_h at the dry end of the investigated tension range,
532 but a smaller one close to saturation (Figure 10).



533

534 **Figure 10: Evolution of weighted mean K_h as a function of applied tension for (a) aridity**
535 **class, (b) potential annual evapotranspiration and (c) mean annual diurnal temperature**
536 **range. The shaded areas and the error bars represent the weighted standard error of the**
537 **mean.**

538 4 Conclusions

539 Our results suggest that climate change will influence soil hydraulic properties near saturation. This
540 may complicate model predictions of water balance in a future climate, particularly the risks of surface
541 runoff, soil erosion and waterlogging. Climatic factors are more strongly correlated to near-saturated
542 hydraulic conductivities than soil texture, bulk density and organic carbon content. At and very close to
543 soil saturation, the correlations between hydraulic conductivity and climate variables vanished,
544 indicating a change in flow paths. Instead, the soil bulk density showed the largest correlation, in line
545 with the fact that more compact soils tend to lack a well-connected macropore system. Hypotheses as
546 to why climate variables are correlated with the hydraulic conductivity were discussed, but these need
547 to be further investigated. Most probably, the impacts of climate are linked to macropore networks
548 associated with biological activity, pedogenesis, and land use. Only a few land use and soil
549 management related factors could be investigated in our study. They were all found to significantly
550 influence K_h , with effect sizes similar to those of soil properties like texture and organic carbon content.
551 Also, experimenter bias as introduced by choice of measurement time relative to soil tillage,
552 experimental design or data evaluation appeared to be as important for the saturated and near-
553 saturated hydraulic conductivity as soil texture or bulk density. There is a need for better documentation



554 and accessibility of measurement data and associated meta-data, as has already been suggested by
 555 others (McBratney et al., 2011; Basche & DeLonge, 2019).

556 5 Appendix A

557 5.1 Data query details

558 **Table A1: Query strings, search engines, number of result pages that were processed and**

559 **dates of the search for finding new data for OTIM**

| Search engine | Query string (time range considered) | Date | Pages |
|----------------|--|------------|-------|
| Google Scholar | hydraulic unsaturated conductivity tillage crop | 2021/06/02 | 12 |
| Google Scholar | tension disk infiltrometer | 2021/06/02 | 3 |
| Web of Science | field unsaturated hydraulic conductivity agriculture | 2021/06/02 | 3 |
| Google Scholar | Near-saturated hydraulic conductivity (2013-2021) | 2021/06/01 | ~8 |
| ISI Web | Near-saturated hydraulic conductivity (2013-2021) | 2021/06/01 | ~8 |
| Scopus | Near-saturated hydraulic conductivity (2013-2021) | 2021/06/01 | ~8 |
| Google Scholar | hydraulic conductivity (2013-2021) | 2021/05/31 | ~8 |
| ISI Web | hydraulic conductivity (2013-2021) | 2021/05/31 | ~8 |
| Scopus | hydraulic conductivity (2013-2021) | 2021/05/31 | ~8 |
| Google Scholar | tension disk infiltrometer (2013-2021) | 2021/05/31 | ~5 |
| ISI Web | tension disk infiltrometer (2013-2021) | 2021/05/31 | ~5 |
| Google Scholar | Near-saturated hydraulic conductivity (2013-2021) | 10/06/2021 | ~8 |
| Google Scholar | tillage hydraulic conductivity (2013-2021) | 10/06/2021 | ~8 |
| Google Scholar | tension disk infiltrometer tillage (2013-2021) | 10/06/2021 | ~8 |
| Scopus | Near-saturated hydraulic conductivity (2013-2021) | 10/06/2021 | ~3 |
| Scopus | tillage hydraulic conductivity (2013-2021) | 10/06/2021 | ~3 |
| Scopus | tension disk infiltrometer (tillage) (2013-2021) | 10/06/2021 | ~3 |
| Scopus | "near-saturated" and infiltration | 18/06/2021 | ~4 |
| Scopus | "mini disk infiltrometer" | 18/06/2021 | ~4 |
| Scopus | "tension infiltrometer" | 23/06/2021 | ~5 |

560

561 5.2 Data rejection

562 **Table A2: Reasons for data rejection.**

| Reason | Number of publications |
|--------------|------------------------|
| no access | 2 |
| not relevant | 19 |



| | |
|----------------------------|----|
| only one tension | 61 |
| overlap with another paper | 3 |
| no data published | 32 |

563

564 **5.3 Database organisation**

565 OTIM is organised in nine individual tables illustrated in Table A3. The main table is named *experiments*.

566 It contains identifiers with which all the other tables are linked. The identifiers are shown in bold font in

567 Table A3. The *reference* table contains information on the references for each study. The *location* table

568 lists the coordinates of the measurement sites. The tables *soilProperties*, *soilManagement* and *climate*

569 store data as implied by their names. The *method* table gives details on the specifications of the tension-

570 disk infiltrometer and the method to calculate hydraulic conductivity from the infiltration rate. The

571 *rawData* table contains the hydraulic conductivities and respective supply tensions as stated in the

572 corresponding source publication. Note that OTIM does not contain raw data for the entries of the

573 original version compiled for Jarvis et al., 2013. Finally, *modelFit* reports K_h for $0 \leq h \leq 100$ mm as

574 described above. For more details, the reader is directed to the 'description' tab of the database (not

575 shown in Table A3) where the meanings and units of each column are explained.

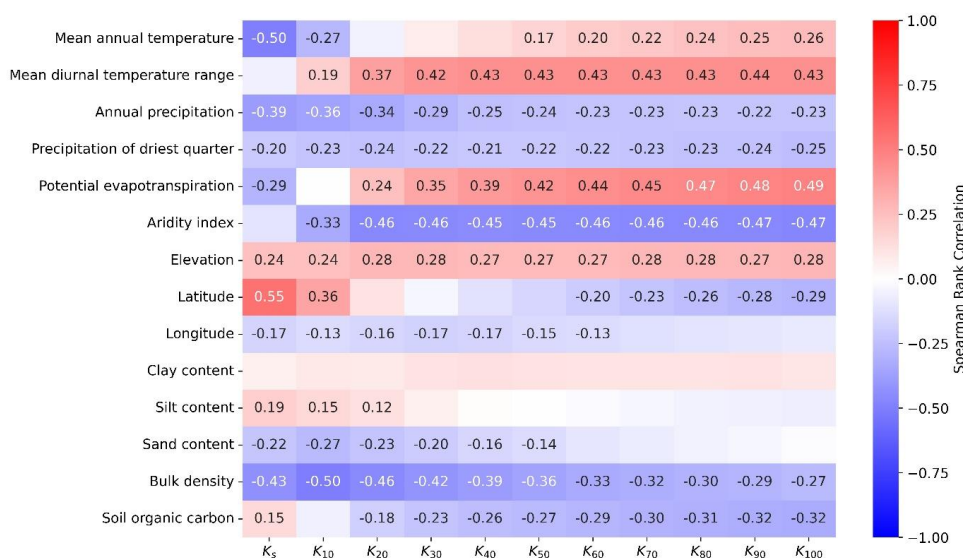
| locations | experiments | method | soilProperties |
|-----------------------------------|--------------------|--------------|---------------------|
| - LocID | - ExpID | - MTFID | - SSPID |
| - Location | - ExpName | - MethodName | - SPName |
| - Latitude | - ReferenceTag | - Month1 | - TextureClass |
| - Longitude | - Location | - Month2 | - SoilTextureUSDA |
| - Comments | - ClimateName | - Season | - SoilTextureFAO |
| | - MethodName | - Reps | - SoilType |
| | - MTFName | - YearExp | - SoilTypeClass |
| | - SPName | - Method | - ClayContent |
| | - SMName | - Direction | - SiltContent |
| | - DatasetAddedBy | - Tmin | - SandContent |
| | - DatasetCheckedBy | - Tmax | - BulkDensity |
| | | - UpperD_m | - SoilOrganicCarbon |
| | | - Diameter | |
| | | - Diameter2 | |
| | | - Diameter3 | |
| | | - Comment | |
| climate | reference | modelFit | soilManagement |
| - ClimateName | - RefID | - MTFName | - SMName |
| - AnnualMeanTemperature | - ReferenceTag | - Ks | - Landuse |
| - MeanTemperatureofWarmestQuarter | - ReferenceYear | - Kunsat | - LanduseClass |
| - MeanTemperatureofColdestQuarter | - ReferenceName | - slope | - Tillage |
| - AnnualPrecipitation | - ReferenceDOI | - R2 | - TillageClass |
| - PrecipitationofWettestMonth | - ReferenceTitle | - Hmin | - NbOfCropRotation |
| - PrecipitationofDriestMonth | - Comments | - Intercept | - CurrentCrop |
| - PrecipitationofWettestQuarter | | - K1 | - CropClass |
| - PrecipitationofDriestQuarter | | - K2 | - CropRotation |
| - PrecipitationofWarmestQuarter | | - K3 | - CoverCrop |
| - PrecipitationofColdestQuarter | | - K4 | - CoverCropClass |
| - MeanDiurnalRange | | - K5 | - Residue |
| - Isothermality | | - K6 | - ResidueClass |
| - TemperatureSeasonality | | - K7 | - Grazing |
| - MaxTemperatureofWarmestMonth | | - K8 | - GrazingClass |
| - MinTemperatureofColdestMonth | | - K9 | - Irrigation |
| - TemperatureAnnualRange | | - K10 | - IrrigationClass |
| - MeanTemperatureofWettestQuarter | | | - Residue |
| - MeanTemperatureofDriestQuarter | | | - ResidueClass |
| - elevation | | | - Grazing |
| - AverageAridityIndex | | | - GrazingClass |
| - AverageAnnualEvapoTranspiration | | | - Irrigation |
| - AridityClass | | | - IrrigationClass |
| | | | - Compaction |
| | | | - CompactionClass |
| | | | - OtherAmendments |
| | | | - AmendmentClass |
| | | | - SamplingTime |
| | | | - SamplingTimeClass |
| | | | - Comments |

576



577 **Table A3: Structure of the OTIM database with its different tables and columns. In the**
 578 **soilManagement table, the columns with the suffix “Class” denote columns in which the**
 579 **data reported in the source publications were summarised into classes to facilitate**
 580 **comparing them. For example, the reported CurrentCrop like wheat, rye, barley or oat was**
 581 **assigned the CropClass cereals. The rows in bold denote unique identifiers with which the**
 582 **table entries are linked to the experiments table.**

583 **6 Appendix B**



584

585 **Table B1: Weighted Spearman rank correlation coefficients between K_h at different**
 586 **tensions and climatic features, soil properties, land use and management factors and**
 587 **methodological details. In contrast to Table 6, only the 193 data entries from arable fields**
 588 **using a dry-to-wet sequence and the steady-state piecewise method (Reynolds and Elrick,**
 589 **1991; Ankeny et al., 1991) were considered. Correlation coefficients are shown up to p-**
 590 **values of 0.001.**

591 **7 Code availability**



592 All scripts used to compile this study are publically available in form of Jupyter notebooks on GitHub:
593 <https://github.com/climasoma/OTIM> and <https://github.com/climasoma/machine-learning>.

594 8 Data availability

595 The OTIM database is available from the BONARES data repository
596 <https://tools.bonares.de/doi/datasets>.

597 9 Author contribution

598 Funding acquisition: JK, SG; project administration, supervision and conceptualization: JK; meta-
599 database collation and validation: LA, GuBl, JK; Python code development, including visualization:
600 GuBl, JK; applying statistical analyses and writing original manuscript draft: GuBl, JK; Reviewing and
601 editing the manuscript: JK, NJ, SG; GiBr, GuBl.

602 10 Competing interests

603 11 The authors declare that they have no conflict of interest.

604 12 Acknowledgements

605 This study was carried out in the framework of the EJP Soil ClimaSoMa project, which has received
606 funding from the EU Horizon 2020 Research and Innovation programme under grant number 862695.
607 We thank Lionel Alletto, Mats Larsbo, Ali Meshgi and Wim Cornelis for sharing additional details to their
608 source publication.

609 13 References

610 Alagna, V., Bagarello, V., Di Prima, S., and Iovino, M.: Determining hydraulic properties of a loam soil
611 by alternative infiltrometer techniques: Hydraulic Properties of a Loam Soil by Infiltration Techniques,
612 *Hydrol. Process.*, 30, 263–275, <https://doi.org/10.1002/hyp.10607>, 2016.



- 613 Alletto, L., Pot, V., Giuliano, S., Costes, M., Perdrieux, F., and Justes, E.: Temporal variation in soil
614 physical properties improves the water dynamics modeling in a conventionally-tilled soil, *Geoderma*,
615 243–244, 18–28, <https://doi.org/10.1016/j.geoderma.2014.12.006>, 2015.
- 616 Angulo-Jaramillo, R., Vandervaere, J. P., Roulier, S., Thony, J. L., Gaudet, J. P., and Vauclin, M.: Field
617 measurement of soil surface hydraulic properties by disc and ring infiltrometers - A review and recent
618 developments, *Soil Tillage Res.*, 55, 1–29, 2000.
- 619 Ankeny, M. D., Ahmed, M., Kaspar, T. C., and Horton, R.: Simple field method for determining
620 unsaturated hydraulic conductivity, 55, 467–470, 1991.
- 621 Bagarello, V., Baiamonte, G., Castellini, M., Di Prima, S., and Iovino, M.: A comparison between the
622 single ring pressure infiltrometer and simplified falling head techniques: COMPARING PRESSURE
623 INFILTRMETER AND SFH TECHNIQUES, *Hydrol. Process.*, 28, 4843–4853,
624 <https://doi.org/10.1002/hyp.9980>, 2014.
- 625 Baranian Kabir, E., Bashari, H., Bassiri, M., and Mosaddeghi, M. R.: Effects of land-use/cover change
626 on soil hydraulic properties and pore characteristics in a semi-arid region of central Iran, *Soil and Tillage
627 Research*, 197, 104478, <https://doi.org/10.1016/j.still.2019.104478>, 2020.
- 628 Basche, A. D. and DeLonge, M. S.: Comparing infiltration rates in soils managed with conventional and
629 alternative farming methods: A meta-analysis, 14, <https://doi.org/10.1371/journal.pone.0215702>, 2019.
- 630 Bártková, K., Miháliková, M., and Matula, S.: Hydraulic Properties of a Cultivated Soil in Temperate
631 Continental Climate Determined by Mini Disk Infiltrometer, *Water*, 12, 843,
632 <https://doi.org/10.3390/w12030843>, 2020.
- 633 Bodner, G., Scholl, P., Loiskandl, W., and Kaul, H. P.: Environmental and management influences on
634 temporal variability of near saturated soil hydraulic properties, 204, 120–129,
635 <https://doi.org/10.1016/j.geoderma.2013.04.015>, 2013.



- 636 Bottinelli, N., Menasseri-Aubry, S., Cluzeau, D., and Hallaire, V.: Response of soil structure and
637 hydraulic conductivity to reduced tillage and animal manure in a temperate loamy soil, *Soil Use Manage*,
638 29, 401–409, <https://doi.org/10.1111/sum.12049>, 2013.
- 639 Bouma, J.: Using soil survey data for quantitative land evaluation, 9, 177–213, 1989.
- 640 Capowiez, Y., Sammartino, S., Keller, T., and Bottinelli, N.: Decreased burrowing activity of endogeic
641 earthworms and effects on water infiltration in response to an increase in soil bulk density, *Pedobiologia*,
642 85-86, 150728, 2021.
- 643 Costa, J. L., Aparicio, V., and Cerdà, A.: Soil physical quality changes under different management
644 systems after 10 years in the Argentine humid pampa, *Solid Earth*, 6, 361–371,
645 <https://doi.org/10.5194/se-6-361-2015>, 2015.
- 646 De Boever, M., Gabriels, D., Ouessar, M., and Cornelis, W.: Influence of Acacia Trees on Near-Surface
647 Soil Hydraulic Properties in Arid Tunisia, *Land Degrad. Develop.*, 27, 1805–1812,
648 <https://doi.org/10.1002/ldr.2302>, 2016.
- 649 Etana, A., Larsbo, M., Keller, T., Arvidsson, J., Schjønning, P., Forkman, J., and Jarvis, N.: Persistent
650 subsoil compaction and its effects on preferential flow patterns in a loamy till soil, *Geoderma*, 192, 430–
651 436, <https://doi.org/10.1016/j.geoderma.2012.08.015>, 2013.
- 652 Fashi, F. H., Gorji, M., and Sharifi, F.: THE USE OF SOIL HYDRAULIC PROPERTIES AS
653 INDICATORS FOR ASSESSING THE IMPACT OF MANAGEMENT PRACTICES UNDER SEMI-ARID
654 CLIMATES, *Environ. Eng. Manag. J.*, 18, 1057–1066, <https://doi.org/10.30638/eemi.2019.102>, 2019.
- 655 Fasinmirin, J. T., Olorunfemi, I. E., and Olakuleyin, F.: Strength and hydraulics characteristics variations
656 within a tropical Alfisol in Southwestern Nigeria under different land use management, *Soil and Tillage
657 Research*, 182, 45–56, <https://doi.org/10.1016/j.still.2018.04.017>, 2018.
- 658 Greenwood: Land use and tillage effects on soil saturated hydraulic conductivity: Does infiltration
659 method matter?, Master Thesis, Lincoln University, New-Zeeland, 2017.



- 660 Fick, S. E. and Hijmans, R. J.: WorldClim 2: new 1-km spatial resolution climate surfaces for global land
661 areas, 37, 4302–4315, <https://doi.org/10.1002/joc.5086>, 2017.
- 662 Gupta, S., Hengl, T., Lehmann, P., Bonetti, S., and Or, D.: SoilKsatDB: global database of soil saturated
663 hydraulic conductivity measurements for geoscience applications, 13, 1593–1612,
664 <https://doi.org/10.5194/essd-13-1593-2021>, 2021a.
- 665 Gupta, S., Lehmann, P., Bonetti, S., Papritz, A., and Or, D.: Global Prediction of Soil Saturated
666 Hydraulic Conductivity Using Random Forest in a Covariate-Based GeoTransfer Function (CoGTF)
667 Framework, 13, e2020MS002242, <https://doi.org/10.1029/2020MS002242>, 2021b.
- 668 Hallam, J., Berdeni, D., Grayson, R., Guest, E. J., Holden, J., Lappage, M. G., Prendergast-Miller, M.
669 T., Robinson, D. A., Turner, A., Leake, J. R., and Hodson, M. E.: Effect of earthworms on soil physico-
670 hydraulic and chemical properties, herbage production, and wheat growth on arable land converted to
671 ley, *Science of The Total Environment*, 713, 136491, <https://doi.org/10.1016/j.scitotenv.2019.136491>,
672 2020.
- 673 Hardie, M. A., Doyle, R. B., Cotching, W. E., Mattern, K., and Lisson, S.: Influence of antecedent soil
674 moisture on hydraulic conductivity in a series of texture-contrast soils: INFLUENCE OF ANTECEDENT
675 SOIL MOISTURE ON HYDRAULIC CONDUCTIVITY, *Hydrol. Process.*, 26, 3079–3091,
676 <https://doi.org/10.1002/hyp.8325>, 2012.
- 677 Hillel, D.: *Introduction to Environmental Soil Physics*, Academic Press, Amsterdam, 2004.
- 678 Hirmas, D. R., Giménez, D., Nemes, A., Kerry, R., Brunsell, N. A., and Wilson, C. J.: Climate-induced
679 changes in continental-scale soil macroporosity may intensify water cycle, 561, 100–103,
680 <https://doi.org/10.1038/s41586-018-0463-x>, 2018.
- 681 Holden, J., Wearing, C., Palmer, S., Jackson, B., Johnston, K., and Brown, L. E.: Fire decreases near-
682 surface hydraulic conductivity and macropore flow in blanket peat: FIRE AND BLANKET PEAT
683 HYDROLOGY, *Hydrol. Process.*, 28, 2868–2876, <https://doi.org/10.1002/hyp.9875>, 2014.



- 684 Hyväluoma, J., Rätty, M., Kaseva, J., and Keskinen, R.: Changes over time in near-saturated hydraulic
685 conductivity of peat soil following reclamation for agriculture, 34, 237–243,
686 <https://doi.org/10.1002/hyp.13578>, 2020.
- 687 Iovino, M., Castellini, M., Bagarello, V., and Giordano, G.: Using Static and Dynamic Indicators to
688 Evaluate Soil Physical Quality in a Sicilian Area: SOIL PHYSICAL QUALITY EVALUATION BY STATIC
689 AND DYNAMIC INDICATORS, Land Degrad. Develop., 27, 200–210, <https://doi.org/10.1002/ldr.2263>,
690 2016.
- 691 IUSS Working Group WRB: World Reference Base for Soil Resources 2014, Update 2015. International
692 Soil Classification System for Naming Soils and Creating Legends for Soil Maps., FAO, Rome, 2015.
- 693 Jarvis, N., Koestel, J., Messing, I., Moeys, J., and Lindahl, A.: Influence of soil, land use and climatic
694 factors on the hydraulic conductivity of soil, 17, 5185–5195, <https://doi.org/10.5194/hess-17-5185-2013>,
695 2013.
- 696 Jorda, H., Bechtold, M., Jarvis, N., and Koestel, J.: Using boosted regression trees to explore key
697 factors controlling saturated and near-saturated hydraulic conductivity, 66, 744–756,
698 <https://doi.org/10.1111/ejss.12249>, 2015.
- 699 Kelishadi, H., Mosaddeghi, M. R., Hajabbasi, M. A., and Ayoubi, S.: Near-saturated soil hydraulic
700 properties as influenced by land use management systems in Koohrang region of central Zagros, Iran,
701 Geoderma, 213, 426–434, <https://doi.org/10.1016/j.geoderma.2013.08.008>, 2014.
- 702 Keskinen, R., Rätty, M., Kaseva, J., and Hyväluoma, J.: Variations in near-saturated hydraulic
703 conductivity of arable mineral topsoils in south-western and central-eastern Finland, AFSci, 28,
704 <https://doi.org/10.23986/afsci.79329>, 2019.
- 705 Khetdan, C., Chittamart, N., Tawornpruek, S., Kongkaew, T., Onsamrarn, W., and Garré, S.: Influence
706 of rock fragments on hydraulic properties of Ultisols in Ratchaburi Province, Thailand, Geoderma
707 Regional, 10, 21–28, <https://doi.org/10.1016/j.geodrs.2017.04.001>, 2017.



- 708 Klute, A. and Dirksen, C.: Hydraulic conductivity and diffusivity: Laboratory measurements, in: Methods
709 of soil analysis, Part 1, vol. 1, edited by: Klute, A., Soil Science Society of America, Inc., Madison,
710 Wisconsin, USA, 687–734, 1986.
- 711 Koestel, J., Dathe, A., Skaggs, T. H., Klakegg, O., Ahmad, M. A., Babko, M., Giménez, D., Farkas, C.,
712 Nemes, A., and Jarvis, N.: Estimating the Permeability of Naturally Structured Soil From Percolation
713 Theory and Pore Space Characteristics Imaged by X-Ray, *Water Resources Research*, 54, 9255–9263,
714 2018.
- 715 Larsbo, M., Koestel, J., and Jarvis, N.: Relations between macropore network characteristics and the
716 degree of preferential solute transport, 18, 5255–5269, <https://doi.org/10.5194/hess-18-5255-2014>,
717 2014.
- 718 Larsbo, M., Sandin, M., Jarvis, N., Etana, A., and Kreuger, J.: Surface Runoff of Pesticides from a Clay
719 Loam Field in Sweden, *J. Environ. Qual.*, 45, 1367–1374, <https://doi.org/10.2134/jeq2015.10.0528>,
720 2016a.
- 721 Larsbo, M., Koestel, J., Kätterer, T., and Jarvis, N.: Preferential transport in macropores is reduced by
722 soil organic carbon, *Vadose Zone Journal*, 15, 2016b.
- 723 Lipiec, J. and Hatano, R.: Quantification of compaction effects on soil physical properties and crop
724 growth, *Geoderma*, 116, 107–136, 2003.
- 725 Logsdon, S. D. and Jaynes, D. B.: Methodology for Determining Hydraulic Conductivity with Tension
726 Infiltrimeters, 57, 1426–1431, <https://doi.org/10.2136/sssaj1993.03615995005700060005x>, 1993.
- 727 Lopes, V. S., Cardoso, I. M., Fernandes, O. R., Rocha, G. C., Simas, F. N. B., de Melo Moura, W.,
728 Santana, F. C., Veloso, G. V., and da Luz, J. M. R.: The establishment of a secondary forest in a
729 degraded pasture to improve hydraulic properties of the soil, *Soil and Tillage Research*, 198, 104538,
730 <https://doi.org/10.1016/j.still.2019.104538>, 2020.



- 731 Lozano, L. A., Germán Soracco, C., Buda, V. S., Sarli, G. O., and Filgueira, R. R.: Stabilization of soil
732 hydraulic properties under a long term no-till system, *Rev. Bras. Ciênc. Solo*, 38, 1281–1292,
733 <https://doi.org/10.1590/S0100-06832014000400024>, 2014.
- 734 Lozano-Baez, S. E., Cooper, M., Frosini de Barros Ferraz, S., Ribeiro Rodrigues, R., Castellini, M., and
735 Di Prima, S.: Assessing Water Infiltration and Soil Water Repellency in Brazilian Atlantic Forest Soils,
736 display, 2020.
- 737 Matula, S., Miháliková, M., Lufinková, J., and Bártková, K.: The role of the initial soil water content in the
738 determination of unsaturated soil hydraulic conductivity using a tension infiltrometer, *Plant Soil Environ.*,
739 61, 515–521, <https://doi.org/10.17221/527/2015-PSE>, 2015.
- 740 McBratney, A. B., Minasny, B., and Tranter, G.: Necessary meta-data for pedotransfer functions, 160,
741 627–629, <https://doi.org/10.1016/j.geoderma.2010.09.023>, 2011.
- 742 Meshgi, A. and Chui, T. F. M.: Analysing tension infiltrometer data from sloped surface using two-
743 dimensional approximation: ANALYSING TENSION INFILTRMETER DATA FROM SLOPED
744 SURFACE, *Hydrological Processes*, 28, 744–752, <https://doi.org/10.1002/hyp.9621>, 2014.
- 745 Messing, I. and Jarvis, N. J.: Seasonal variation in field-saturated hydraulic conductivity in two swelling
746 clay soils in Sweden, 41, 229–237, 1990.
- 747 Messing, I. & Jarvis, N.J.: Temporal variation in the hydraulic conductivity of a tilled clay soil as
748 measured by tension infiltrometers. *Journal of Soil Science*, 44, 11-24, 1993.
- 749 Meurer, K., Barron, J., Chenu, C., Coucheney, E., Fielding, M., Hallett, P., Herrmann, A. M., Keller, T.,
750 Koestel, J., Larsbo, M., Lewan, E., Or, D., Parsons, D., Parvin, N., Taylor, A., Vereecken, H., and Jarvis,
751 N.: A framework for modelling soil structure dynamics induced by biological activity, *Glob. Change Biol.*,
752 26, 5382–5403, <https://doi.org/10.1111/gcb.15289>, 2020.
- 753 Miller, J. J., Beasley, B. W., Drury, C. F., Larney, F. J., Hao, X., and Chanasyk, D. S.: Influence of long-
754 term feedlot manure amendments on soil hydraulic conductivity, water-stable aggregates, and soil



- 755 thermal properties during the growing season, *Can. J. Soil. Sci.*, 98, 421–435,
756 <https://doi.org/10.1139/cjss-2017-0061>, 2018.
- 757 Nemes, A., Schaap, M. G., Leij, F. J., and Wosten, J. H. M.: Description of the unsaturated soil hydraulic
758 database UNSODA version 2.0, 251, 151–162, 2001.
- 759 Pagliai, M., Vignozzi, N., and Pellegrini, S.: Soil structure and the effect of management practices, *Soil
760 & Tillage Research*, 79, 131-143, 2004.
- 761 Poggio, L., de Sousa, L. M., Batjes, N. H., Heuvelink, G. B. M., Kempen, B., Ribeiro, E., and Rossiter,
762 D.: SoilGrids 2.0: producing soil information for the globe with quantified spatial uncertainty, *SOIL*, 7,
763 217-240, 2021.
- 764 Pulido Moncada, M., Helwig Penning, L., Timm, L. C., Gabriels, D., and Cornelis, W. M.: Visual
765 examinations and soil physical and hydraulic properties for assessing soil structural quality of soils with
766 contrasting textures and land uses, *Soil and Tillage Research*, 140, 20–28,
767 <https://doi.org/10.1016/j.still.2014.02.009>, 2014.
- 768 Rahbeh, M.: Characterization of preferential flow in soils near Zarqa river (Jordan) using in situ tension
769 infiltrometer measurements, 7, e8057, <https://doi.org/10.7717/peerj.8057>, 2019.
- 770 Rahmati, M., Weihermüller, L., Vanderborght, J., Pachepsky, Y. A., Mao, L., Sadeghi, S. H., Moosavi,
771 N., Kheirfam, H., Montzka, C., Van Looy, K., Toth, B., Hazbavi, Z., Al Yamani, W., Albalasmeh, A. A.,
772 Alghzawi, M. Z., Angulo-Jaramillo, R., Antonino, A. C. D., Arampatzis, G., Armino, R. A., Asadi, H.,
773 Bamutaze, Y., Batlle-Aguilar, J., Béchet, B., Becker, F., Blöschl, G., Bohne, K., Braud, I., Castellano,
774 C., Cerdà, A., Chalhoub, M., Cichota, R., Císlarová, M., Clothier, B., Coquet, Y., Cornelis, W., Corradini,
775 C., Coutinho, A. P., De Oliveira, M. B., De Macedo, J. R., Durães, M. F., Emami, H., Eskandari, I.,
776 Farajnia, A., Flammini, A., Fodor, N., Gharaibeh, M., Ghavimipannah, M. H., Ghezzehei, T. A., Giertz,
777 S., Hatzigiannakis, E. G., Horn, R., Jiménez, J. J., Jacques, D., Keesstra, S. D., Kelishadi, H., Kiani-
778 Harchegani, M., Kouselou, M., Jha, M. K., Lassabatere, L., Li, X., Liebig, M. A., Lichner, L., López, M.
779 V., Machiwal, D., Mallants, D., Mallmann, M. S., De Oliveira Marques, J. D., Marshall, M. R., Mertens,



- 780 J., Meunier, F., Mohammadi, M. H., Mohanty, B. P., Pulido-Moncada, M., Montenegro, S., Morbidelli,
781 R., Moret-Fernández, D., Moosavi, A. A., Mosaddeghi, M. R., Mousavi, S. B., Mozaffari, H., Nabiollahi,
782 K., Neyshabouri, M. R., Ottoni, M. V., Ottoni Filho, T. B., Pahlavan-Rad, M. R., Panagopoulos, A., Peth,
783 S., Peyneau, P. E., Picciafuoco, T., Poesen, J., Pulido, M., Reinert, D. J., Reinsch, S., Rezaei, M.,
784 Roberts, F. P., Robinson, D., Rodrigo-Comino, J., Rotunno Filho, O. C., Saito, T., et al.: Development
785 and analysis of the Soil Water Infiltration Global database, 10, 1237–1263, [https://doi.org/10.5194/essd-](https://doi.org/10.5194/essd-10-1237-2018)
786 10-1237-2018, 2018.
- 787 Reynolds, W. D. and Elrick, D. E.: Determination of Hydraulic Conductivity Using a Tension Infiltrometer,
788 55, 633–639, <https://doi.org/10.2136/sssaj1991.03615995005500030001x>, 1991.
- 789 Rienzner, M. and Gandolfi, C.: Investigation of spatial and temporal variability of saturated soil hydraulic
790 conductivity at the field-scale, Soil and Tillage Research, 135, 28–40,
791 <https://doi.org/10.1016/j.still.2013.08.012>, 2014.
- 792 Sandin, M., Koestel, J., Jarvis, N., and Larsbo, M.: Post-tillage evolution of structural pore space and
793 saturated and near-saturated hydraulic conductivity in a clay loam soil, 165, 161–168,
794 <https://doi.org/10.1016/j.still.2016.08.004>, 1, 2017.
- 795 Schaap, M. G. and Leij, F. J.: Improved prediction of unsaturated hydraulic conductivity with the
796 Mualem-van Genuchten model, Soil Science Society of America Journal, 64 (3), pp. 843 – 851, 2000.
- 797 Schaap, M. G., Leij, F. J., and van Genuchten, M. T.: ROSETTA: a computer program for estimating
798 soil hydraulic parameters with hierarchical pedotransfer functions, Journal of Hydrology, 251, 163–176,
799 2001.
- 800 Schlüter, S., Albrecht, L., Schwärzel, K., and Kreiselmeyer, J.: Long-term effects of conventional tillage
801 and no-tillage on saturated and near-saturated hydraulic conductivity – Can their prediction be improved
802 by pore metrics obtained with X-ray CT? Geoderma, 361, 2020.
- 803 Smettem, K. R. J. and Clothier, B. E.: Measuring unsaturated sorptivity and hydraulic conductivity using
804 multiple disc permeameters, 40, 563–568, <https://doi.org/10.1111/j.1365-2389.1989.tb01297.x>, 1989.



- 805 Soracco, C. G., Lozano, L. A., Villarreal, R., Palancar, T. C., Collazo, D. J., Sarli, G. O., and Filgueira,
806 R. R.: EFFECTS OF COMPACTION DUE TO MACHINERY TRAFFIC ON SOIL PORE
807 CONFIGURATION, *Rev. Bras. Ciênc. Solo*, 39, 408–415,
808 <https://doi.org/10.1590/01000683rbc20140359>, 2015.
- 809 Soracco, C. G., Villarreal, R., Melani, E. M., Oderiz, J. A., Salazar, M. P., Otero, M. F., Irizar, A. B., and
810 Lozano, L. A.: Hydraulic conductivity and pore connectivity. Effects of conventional and no-till systems
811 determined using a simple laboratory device, *Geoderma*, 337, 1236–1244,
812 <https://doi.org/10.1016/j.geoderma.2018.10.045>, 2019.
- 813 Tóth, B., Weynants, M., Nemes, A., Makó, A., Bilas, G., and Tóth, G.: New generation of hydraulic
814 pedotransfer functions for Europe, 66, 226–238, <https://doi.org/10.1111/ejss.12192>, 2015.
- 815 Trabucco, A. and Zomer, R.: Global Aridity Index and Potential Evapotranspiration (ET₀) Climate
816 Database, <https://doi.org/10.6084/m9.figshare.7504448.v3>, 2019.
- 817 Van Looy, K., Bouma, J., Herbst, M., Koestel, J., Minasny, B., Mishra, U., Montzka, C., Nemes, A.,
818 Pachepsky, Y. A., Padarian, J., Schaap, M. G., Toth, B., Verhoef, A., Vanderborght, J., van der Ploeg,
819 M. J., Weihermuller, L., Zacharias, S., Zhang, Y. G., and Vereecken, H.: Pedotransfer Functions in
820 Earth System Science: Challenges and Perspectives, 55, 1199–1256,
821 <https://doi.org/10.1002/2017rg000581>, 2017.
- 822 Vandervaere, J.-P., Vauclin, M., and Elrick, D. E.: Transient Flow from Tension Infiltrometers II. Four
823 Methods to Determine Sorptivity and Conductivity, 64, 1272–1284,
824 <https://doi.org/10.2136/sssaj2000.6441272x>, 2000.
- 825 Vereecken, H., Weynants, M., Javaux, M., Pachepsky, Y., Schaap, M. G., and Genuchten, M. T. v.:
826 Using pedotransfer functions to estimate the van Genuchten–Mualem soil hydraulic properties: A
827 review, *Vadose Zone Journal*, 9, 795–820, 2010.
- 828 Wang, L., Garré, S., De Cuyper, T., Pollet, S., Cornelis, W. unpublished data.



- 829 Wanniarachchi, D., Cheema, M., Thomas, R., Kavanagh, V., and Galagedara, L.: Impact of Soil
830 Amendments on the Hydraulic Conductivity of Boreal Agricultural Podzols, *Agriculture*, 9, 133,
831 <https://doi.org/10.3390/agriculture9060133>, 2019.
- 832 Weynants, M., Vereecken, H., and Javaux, M.: Revisiting Vereecken pedotransfer functions:
833 Introducing a closed-form hydraulic model, 8, 86–95, <https://doi.org/10.2136/vzj2008.0062>, 2009.
- 834 Weynants, M., Montanarella, L., Toth, G., Arnoldussen, A., Anaya Romero, M., Bilas, G., Borresen, T.,
835 Cornelis, W., Daroussin, J., Feichtinger, F., Gonçalves, M., Hannam, J., Haugen, L., Hennings, V.,
836 Houskova, B., Iovino, M., Javaux, M., Keay, C., Kätterer, T., Kvaerno, S., Laktinova, T., Lamorski, K.,
837 Lilly, A., Mako, A., Matula, S., Morari, F., Nemes, A., Nyborg, Å., Patyka, N., Riley, H., Romano, N.,
838 Schindler, U., Shein, E., Slawinski, C., Strauss, P., Tóth, B., and Woesten, H.: European
839 HYdropedological Data Inventory (EU-HYDI). EUR 26053, Publications Office of the European Union,
840 Luxembourg (Luxembourg). JRC81129., 2013.
- 841 Whalley, W. R., Dumitru, E., and Dexter, A. R.: Biological effects of soil compaction, *Soil and Tillage*
842 *Research*, 35, 53-68, 1995.
- 843 Wösten, J. H. M., Lilly, A., Nemes, A., and le Bas, C.: Development and use of a database of hydraulic
844 properties of European soils, 90, 169–185, 1999.
- 845 Wösten, J. H. M., Pachepsky, Y. A., and Rawls, W. J.: Pedotransfer functions: bridging the gap between
846 available basic soil data and missing soil hydraulic characteristics, 251, 123–150,
847 [https://doi.org/10.1016/S0022-1694\(01\)00464-4](https://doi.org/10.1016/S0022-1694(01)00464-4), 2001.
- 848 Wooding, R. A.: Steady Infiltration from a Shallow Circular Pond, *Water Resources Research*, 4, 1259-
849 1273, 1968.
- 850 Yu, Z., Dong, W., Young, M. H., Li, Y., and Yang, T.: On evaluating characteristics of the solute transport
851 in the arid vadose zone, 52, 50–62, <https://doi.org/10.1111/gwat.12026>, 2014.



- 852 Yusuf, K. O., Ejieji, C. J., and Baiyeri, M. R.: Determination of sorptivity, infiltration rate and hydraulic
853 conductivity of soil using a tension infiltrometer, 10, 99–108, 2018.
- 854 Yusuf, K. O., Obalolu, R. O., Akinleye, G. T., and Adio-Yusuf, S. I.: Determination of Sorptivity,
855 Infiltration Rate and Hydraulic Conductivity of Loamy Sand using Tension Infiltrometer and Double-Ring
856 Infiltrometer, FUOYEJET, 5, <https://doi.org/10.46792/fuoyejiet.v5i2.501>, 2020.
- 857 Zeng, C., Zhang, F., Wang, Q., Chen, Y., and Joswiak, D. R.: Impact of alpine meadow degradation on
858 soil hydraulic properties over the Qinghai-Tibetan Plateau, Journal of Hydrology, 478, 148–156,
859 <https://doi.org/10.1016/j.jhydrol.2012.11.058>, 2013a.
- 860 Zeng, C., Wang, Q., Zhang, F., and Zhang, J.: Temporal changes in soil hydraulic conductivity with
861 different soil types and irrigation methods, Geoderma, 193–194, 290–299,
862 <https://doi.org/10.1016/j.geoderma.2012.10.013>, 2013b.
- 863 Zhang, R.: Determination of Soil Sorptivity and Hydraulic Conductivity from the Disk Infiltrometer, 61,
864 1024–1030, <https://doi.org/10.2136/sssaj1997.03615995006100040005x>, 1997.
- 865 Zhang, Y., Zhao, W., Li, X., Jia, A., and Kang, W.: Contribution of soil macropores to water infiltration
866 across different land use types in a desert–oasis ecoregion, Land Degrad Dev, 32, 1751–1760,
867 <https://doi.org/10.1002/ldr.3823>, 2021.
- 868 Zhang, Z., Lin, L., Wang, Y., and Peng, X.: Temporal change in soil macropores measured using tension
869 infiltrometer under different land uses and slope positions in subtropical China, J Soils Sediments, 16,
870 854–863, <https://doi.org/10.1007/s11368-015-1295-z>, 2016.
- 871 Zhang, Z. B., Zhou, H., Zhao, Q. G., Lin, H., and Peng, X.: Characteristics of cracks in two paddy soils
872 and their impacts on preferential flow, Geoderma, 228–229, 114–121,
873 <https://doi.org/10.1016/j.geoderma.2013.07.026>, 2014.



- 874 Zhang, Z.-H., Li, X.-Y., Jiang, Z.-Y., Peng, H.-Y., Li, L., and Zhao, G.-Q.: Changes in some soil
875 properties induced by re-conversion of cropland into grassland in the semiarid steppe zone of Inner
876 Mongolia, China, *Plant Soil*, 373, 89–106, <https://doi.org/10.1007/s11104-013-1772-3>, 2013.
- 877 Zhao, X., Wu, P., Gao, X., Tian, L., and Li, H.: Changes of soil hydraulic properties under early-stage
878 natural vegetation recovering on the Loess Plateau of China, *CATENA*, 113, 386–391,
879 <https://doi.org/10.1016/j.catena.2013.08.023>, 2014.
- 880 Zhou, B. B., Wang, Q. J., and Wu, X. B.: Optimal disc tension infiltrometer estimation techniques for
881 hydraulic properties of soil under different land uses, 9, 92–98,
882 <https://doi.org/10.3965/j.ijabe.20160904.2161>, 2016.
- 883 کریمی‌بان, ن.: اثر روش‌های خاک‌ورزی و مدیریت بقایای گیاهی and میرزاوند, ج., موسوی, س. ع., ا., ثامن, ع., افضل‌ی‌نیا, ص
884 برهدایت هیدرولیکی غیر اشباع خاک در تناوب گندم – ذرت, مجله پژوهش‌های حفاظت آب و خاک, 23
885 <https://doi.org/10.22069/jwfst.2016.3190>, 2016.